

Journal of Drug Discovery and Therapeutics

Available Online at www.jddt.in

CODEN: - JDDTBP (Source: - American Chemical Society)

Volume 13, Issue 03; 2025, 97-164

DESIGN AND IN SILICO STUDIES OF TRIAZOLE DERIVATIVES FOR ANTI-TB EFFICACY

Mansi Shastri¹ and Deshbandhu Joshi²¹Department of Pharmaceutical Chemistry, Shrinathji Institute of Pharmacy, Upali Oden Nathdwara-313301, District- Rajsamand, Rajasthan (India)²Professor, Department of Pharmaceutical Chemistry, Shrinathji Institute of Pharmacy, Upali Oden Nathdwara-313301, District- Rajsamand, Rajasthan (India)

Received: 14-04-2025 / Revised: 21-05-2025 / Accepted: 22-06-2025

Corresponding author: Miss Mansi Shastri

Conflict of interest: No conflict of interest.

Abstract:

Tuberculosis (TB), caused by *Mycobacterium tuberculosis*, continues to pose a serious global health threat, especially with the rise in drug-resistant strains. In an effort to discover new and effective treatment options, this study focused on the design and computer-based (in silico) evaluation of triazole derivatives for their potential anti-TB properties. The compounds were tested through molecular docking techniques to explore how well they could bind to important TB-related enzymes such as InhA and DprE1. The isoniazide was used as a reference, since its crystallographic structure bound to oxidoreductase is available under PDB ID: 5JFO used and retrieved from RCSB. The molecular modelling studies were performed using SYBYL X2.0 software (Tripos) running on a core-2 duo Intel processor workstation. The molecules to be analysed were aligned on an appropriate template, which is considered to be common substructure. Some of the designed molecules demonstrated strong binding potential and promising safety profiles, making them good candidates for further development. Overall, the study supports the value of using computational tools in the early stages of TB drug discovery.

1. INTRODUCTION

Tuberculosis (TB) remains one of the leading causes of death from infectious diseases worldwide, primarily caused by *Mycobacterium tuberculosis*. Despite the availability of anti-TB therapies, the emergence of multidrug-resistant (MDR) and extensively drug-resistant (XDR) strains has significantly reduced the effectiveness of existing treatment regimens. This growing resistance highlights the urgent need to discover and develop new, potent, and safe anti-TB agents with novel mechanisms of action. Heterocyclic compounds, particularly triazoles, have attracted considerable attention in medicinal chemistry due to their broad spectrum of biological activities, including antimicrobial,

antifungal, anticancer, and anti-inflammatory properties. The triazole moiety, known for its metabolic stability and ability to interact with various biological targets, has been incorporated into several clinically useful drugs. Given their pharmacological potential, triazole derivatives are promising candidates for the development of novel anti-TB agents. In recent years, computational methods have played a crucial role in drug discovery and development. In silico approaches such as molecular docking, pharmacokinetic profiling, and ADMET prediction enable rapid screening and optimization of lead compounds, significantly reducing time and cost compared to traditional experimental techniques. These tools allow

researchers to predict the binding efficiency of small molecules with biological targets and assess their drug-likeness early in the design phase.

The present study focuses on the design and in silico evaluation of novel triazole derivatives as potential anti-TB agents. Molecular docking studies were conducted against key enzymes involved in *M. tuberculosis* survival and replication, such as InhA and DprE1. Furthermore, ADMET and drug-likeness analyses were performed to identify promising candidates for further synthesis and biological testing. This integrated computational approach aims to provide valuable insights for the development of new anti-TB drugs.

2. MATERIALS AND METHODS

The experimental phase of this study involved molecular modeling and computational analysis to identify potential triazole-based inhibitors targeting the *M. tuberculosis* enoyl-acyl carrier protein reductase (InhA), an essential enzyme in mycolic acid biosynthesis.

A dataset of 46 known oxidoreductase inhibitors was obtained from literature (Zhang et al., 2017), and their IC₅₀ values were converted into pIC₅₀ for 3D-QSAR modeling.

The molecules were aligned using SYBYL-X 2.0 software, and structural optimization was performed. The dataset was divided into training (82 compounds) and test (28 compounds) sets based on structural diversity and activity range

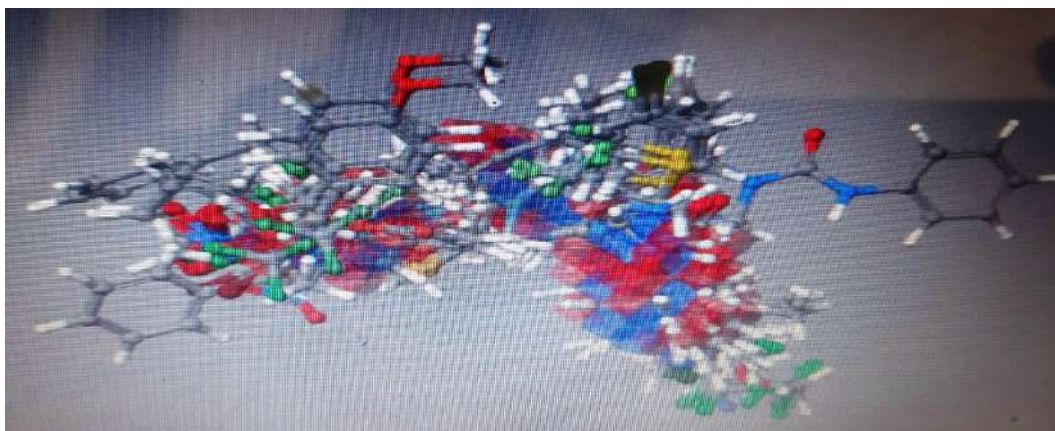


Figure 1: Alignment of all selected molecules

3D-QSAR models (CoMFA and CoMSIA) were generated using different grid spacings and evaluated for steric, electrostatic, hydrophobic, hydrogen bond donor, and acceptor fields. Default probe atoms and grid parameters were applied, with column filtering used to enhance data quality.

Hologram QSAR (HQSAR) models were developed without requiring molecular alignment, using varying fragment distinctions (A, B, C, Ch, H, D), fragment sizes (4–7), and optimal component numbers.

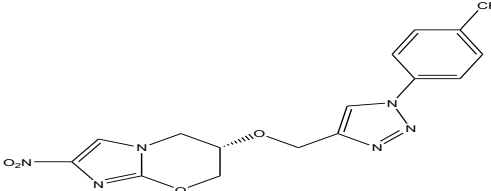
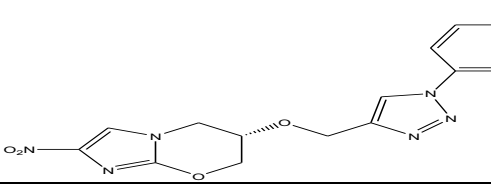
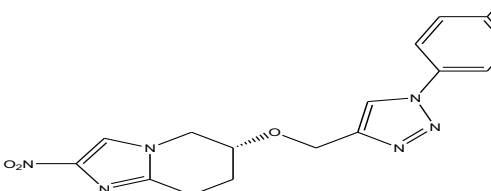

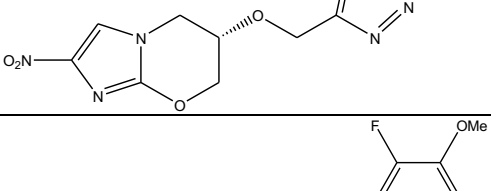
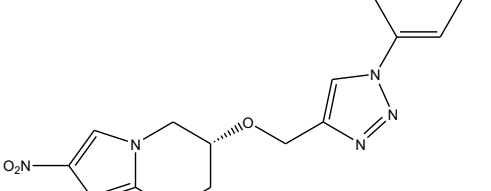
Partial Least Squares (PLS) regression was used to correlate molecular descriptors with biological activity, and model performance was validated using cross-validation (q^2), external test set prediction (r^2_{pred}), and standard error estimation. Contour maps were generated to visualize key structure-activity relationships.

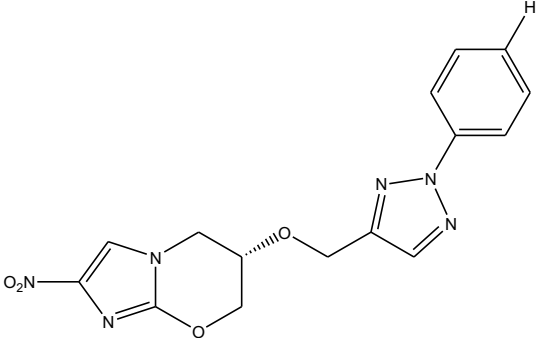
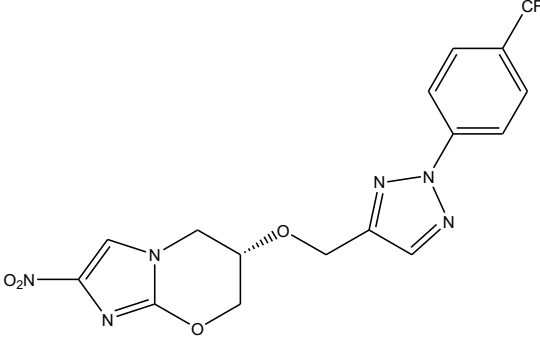
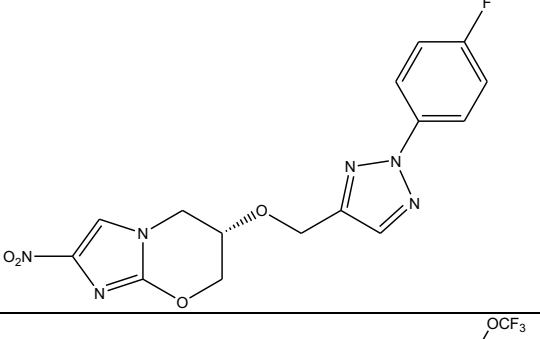
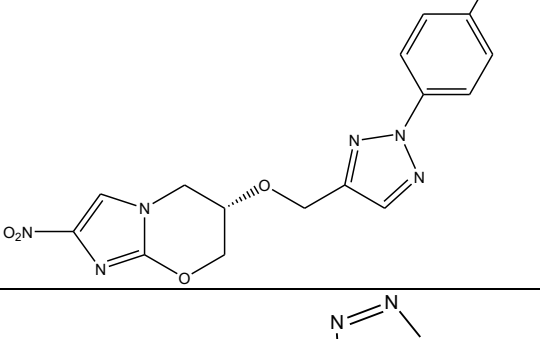
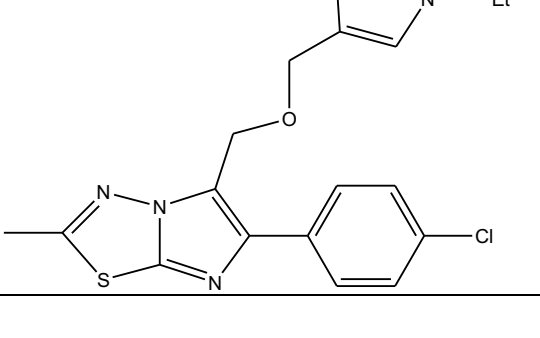
Molecular docking was carried out using Schrödinger Maestro (2016) against the InhA enzyme (PDB ID: 5JFO), and docking protocols were validated by re-docking known inhibitors. Docking interactions and binding affinities were analyzed for all designed compounds.

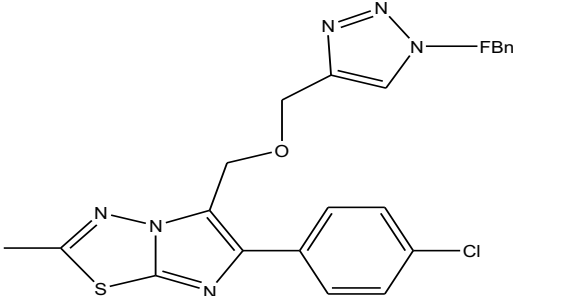
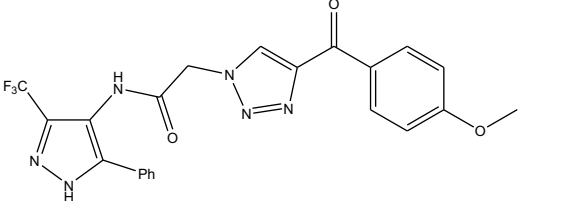
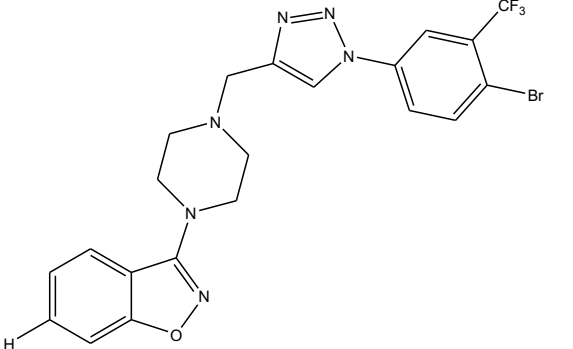
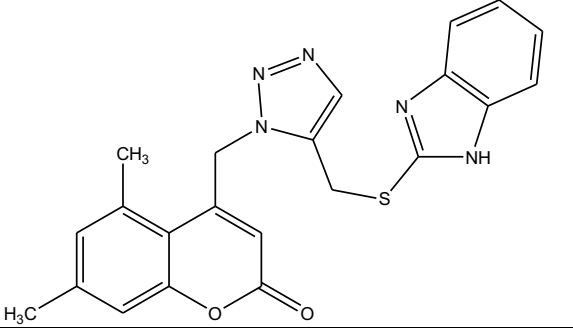
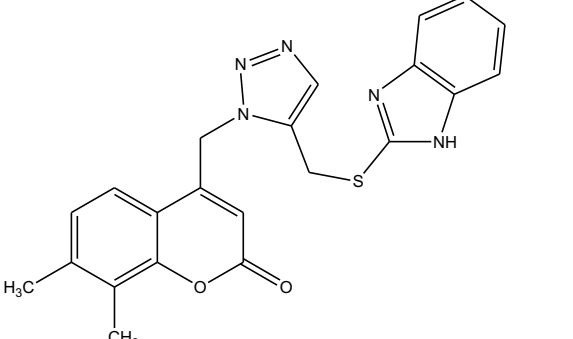
Pharmacophore modeling was conducted using GALAHAD, employing MMFF94 force fields and genetic algorithms to derive models from aligned datasets. Validation was performed using internal test sets.

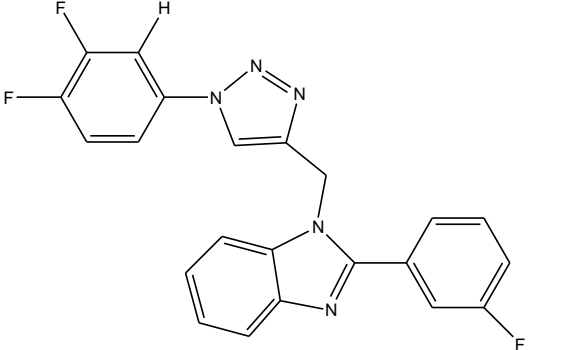
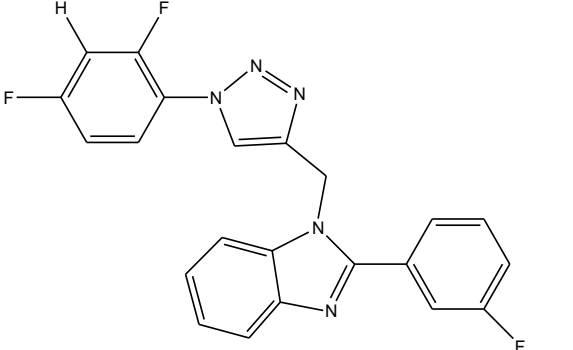
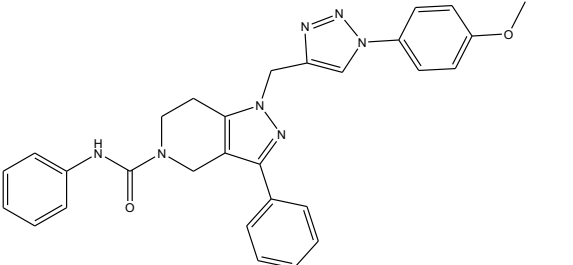
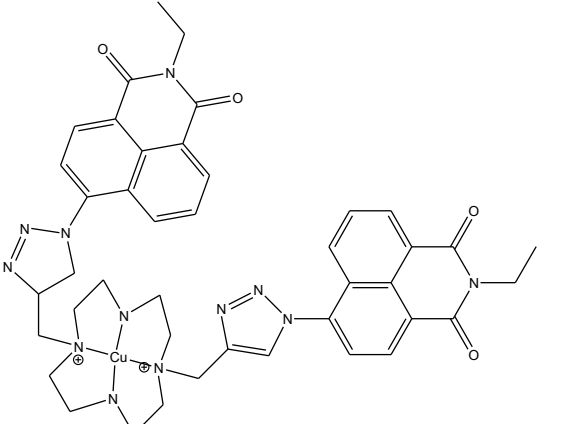
Based on SAR, QSAR, and docking results, 102 novel triazole derivatives were designed. These compounds were further subjected to CoMFA, CoMSIA, HQSAR, and docking analyses to identify promising candidates. The most active candidates exhibited high predicted pIC₅₀ values and favorable docking scores.

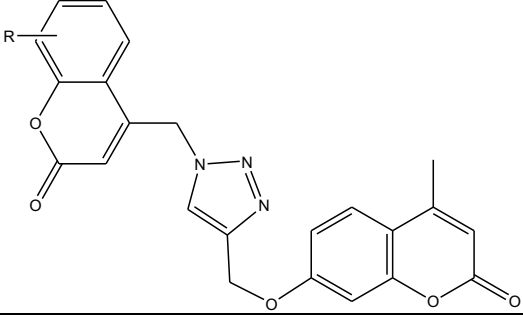
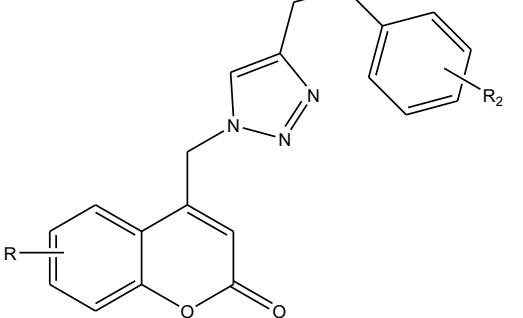
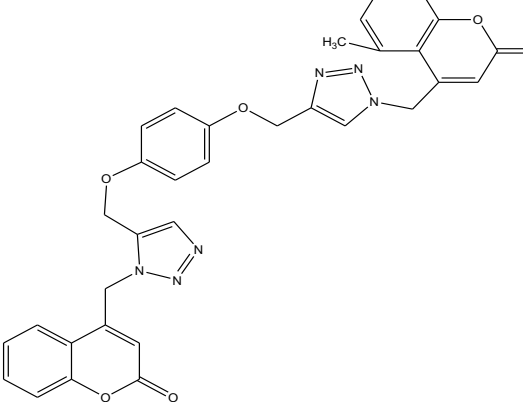
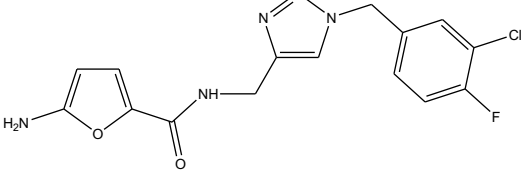
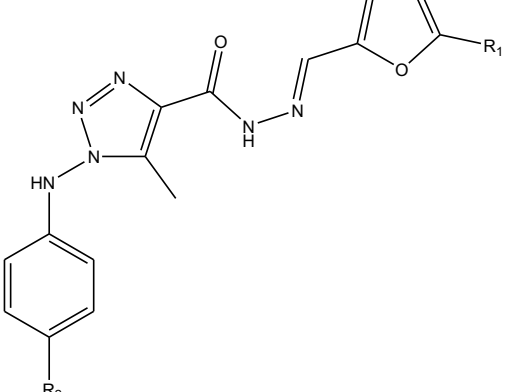
Table 1: Designed Triazole analogues on the basis of computational studies with their predicted data:

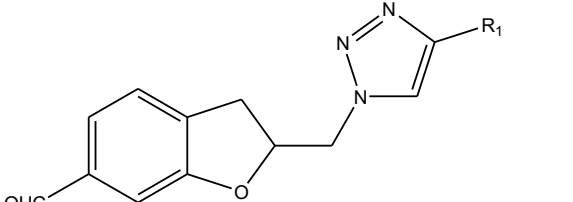
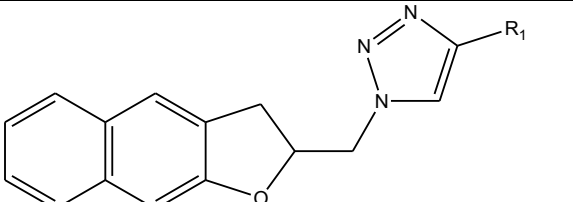
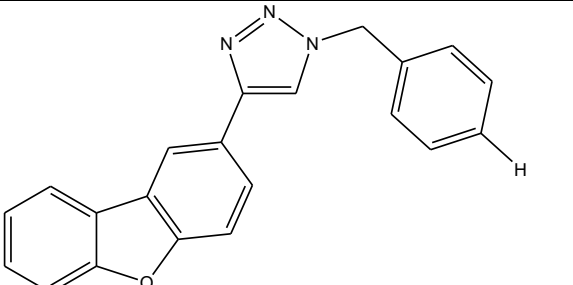
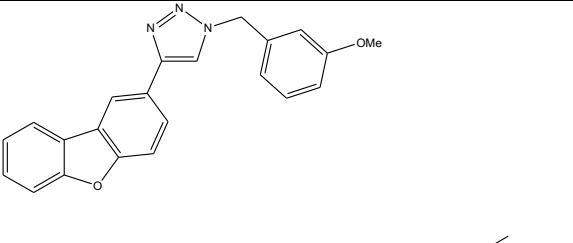
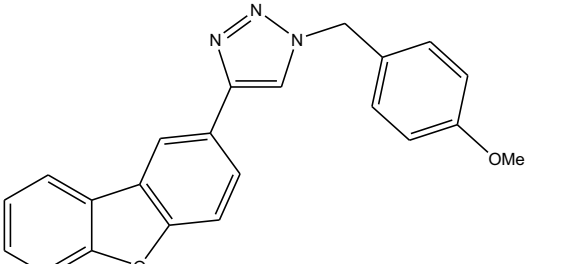
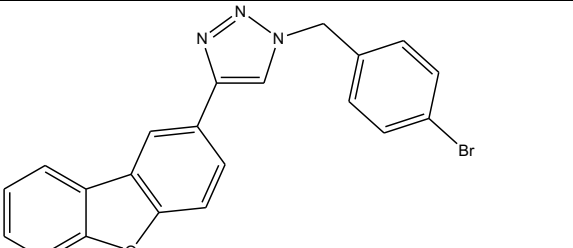
Compound d	Compound structure	Pred pIC ₅₀		HQSA R	Dockin g Score
		CoMF A	CoMSI A		
1		4.3521	4.4758	4.282	4.5033
2		4.3484	4.4751	5.03	3.8241
3		4.3438	4.4782	4.328	3.6918
4		4.3534	4.4803	3.836	5.3139
5		4.3477	4.4731	4.696	5.4296
6		4.3456	4.4747	4.915	3.0611

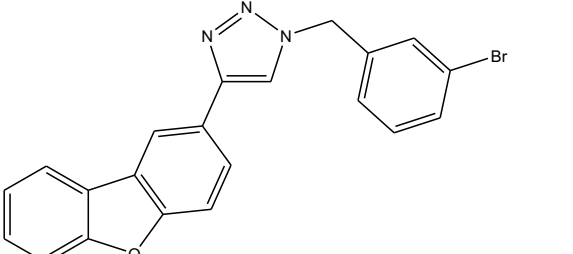
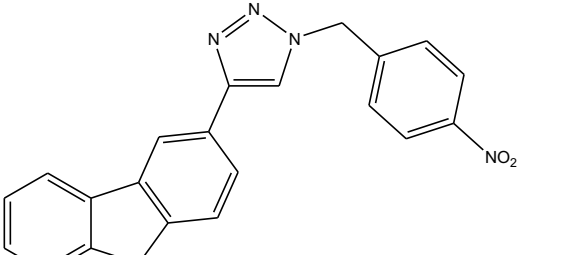
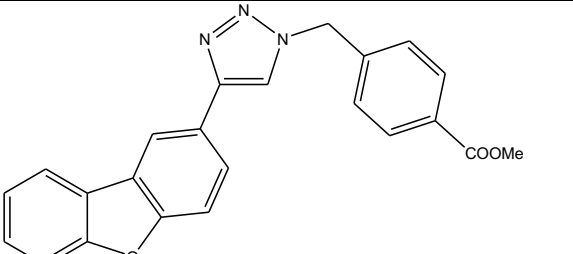
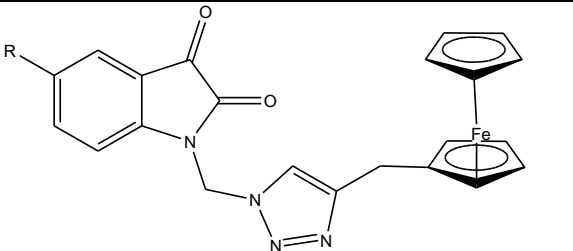
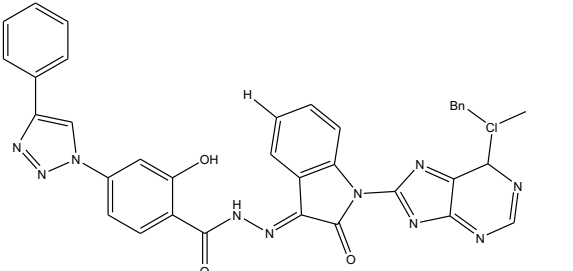
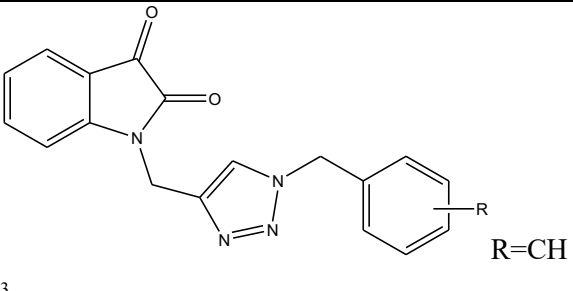
7		4.3488	4.4753	4.578	4.3919
8		4.3493	4.4782	4.447	4.9245
9		4.3486	4.4808	4.425	2.9629
10		4.3502	4.4784	4.756	3.8114
11		4.3511	4.4776	4.503	2.3645

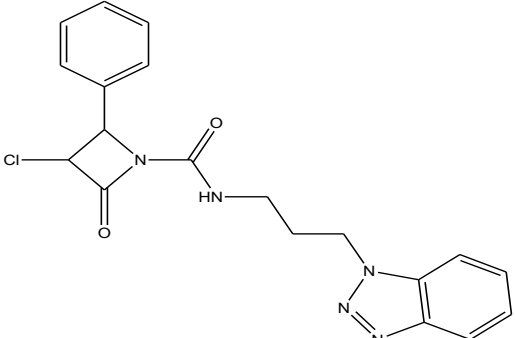
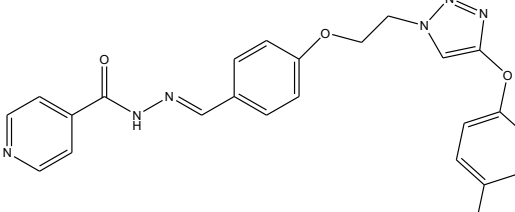
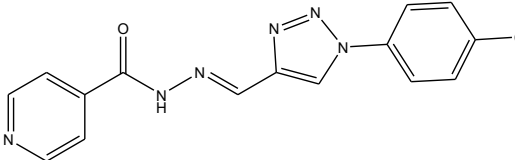
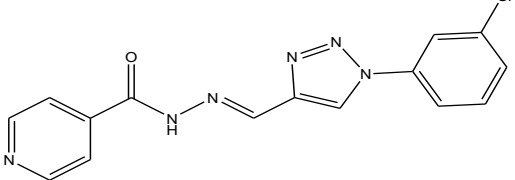
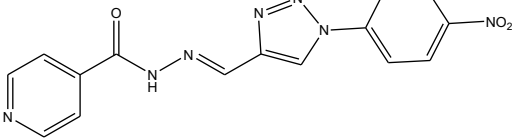
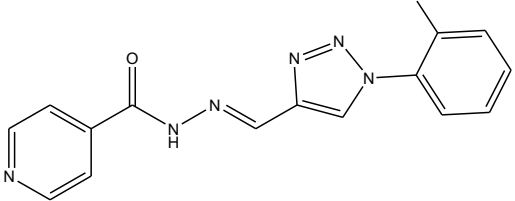
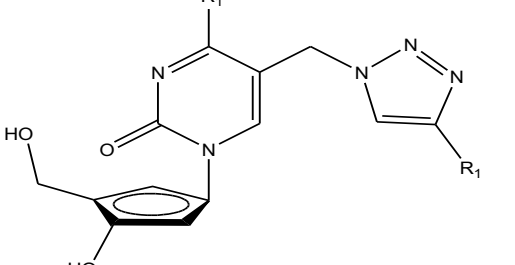
Shastri <i>et al.</i>	Journal of Drug Discovery and Therapeutics (JDDT)				
12		4.3450	4.4755	4.518	5.3367
13		4.3493	4.4778	4.341	5.9438
14		4.3443	4.4748	4.594	4.8035
15		4.3536	4.4984	5.123	6.0693
16		4.3456	4.4717	4.597	2.7969

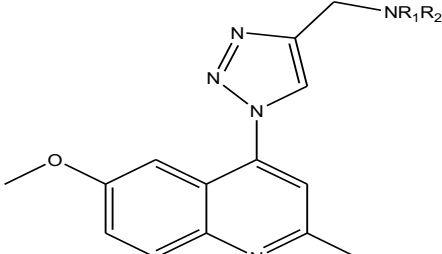
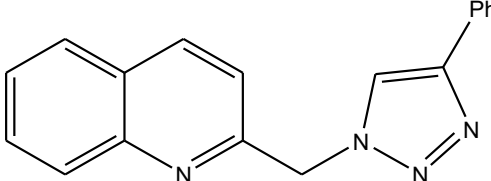
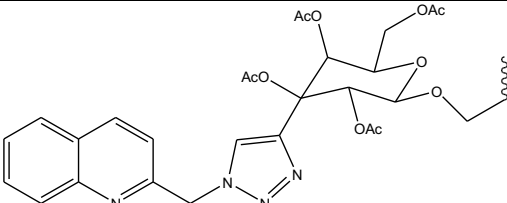
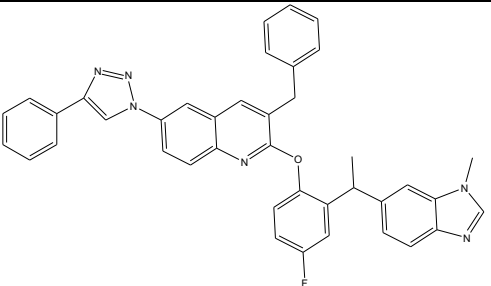
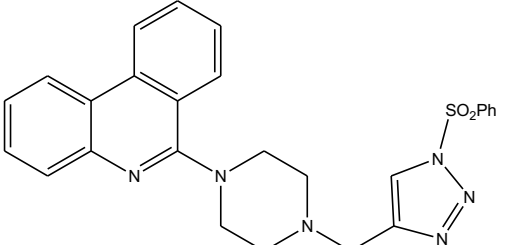
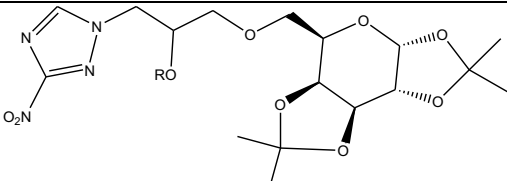
Shastri <i>et al.</i>	Journal of Drug Discovery and Therapeutics (JDDT)				
17		4.3462	4.4732	4.725	4.5086
18		4.3469	4.4785	4.691	4.7630
19		4.3495	4.4753	4.823	3.3900
20		4.3480	4.4792	4.941	3.0896

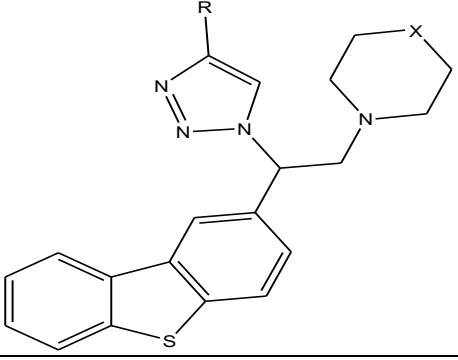
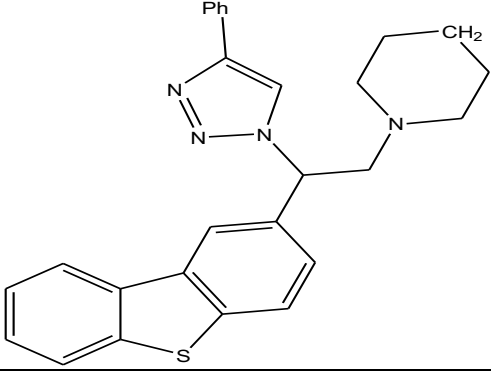
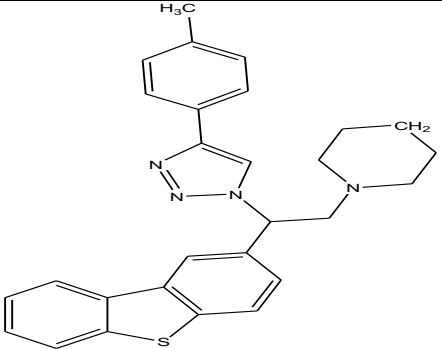
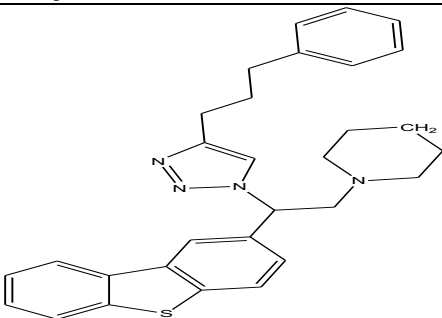
21		4.3461	4.4752	4.647	2.8599
22		4.3492	4.4802	4.518	4.9646
23		4.3465	4.4702	4.866	6.6412
24		4.3452	4.4737	4.826	4.7953
25		4.3467	4.4783	4.742	5.2871

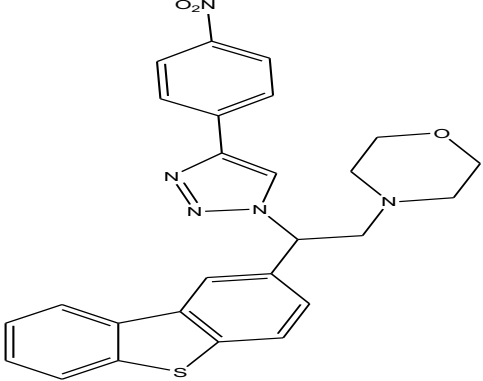
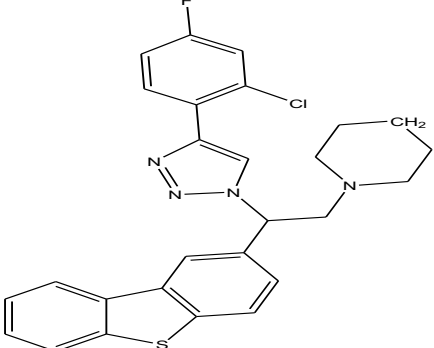
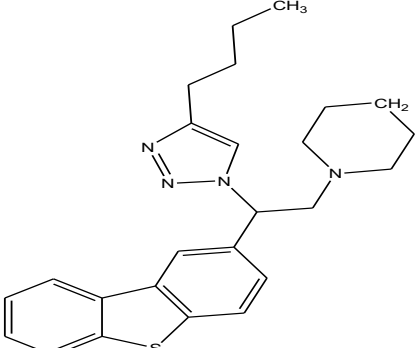
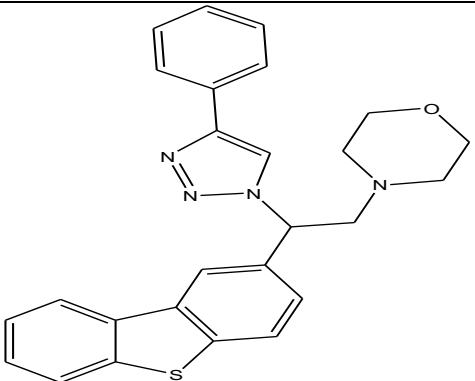
Shastri <i>et al.</i>	Journal of Drug Discovery and Therapeutics (JDDT)				
26		4.3453	4.4697	4.884	6.3892
27		4.3514	4.791	4.373	8.2615
28		4.3473	4.4783	4.293	5.4088
29		4.3470	4.4761	4.939	6.3040
30		4.3431	4.4754	4.775	4.8325
31		4.3454	4.4758	4.555	4.9260

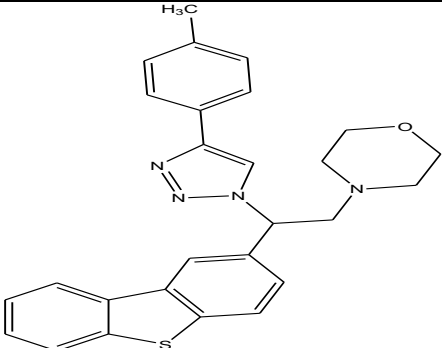
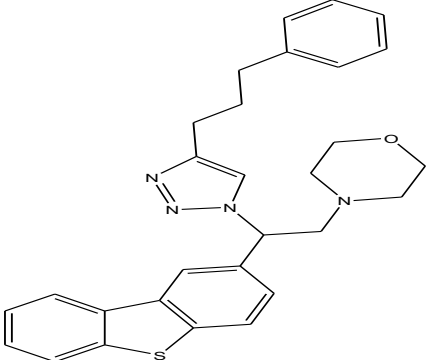
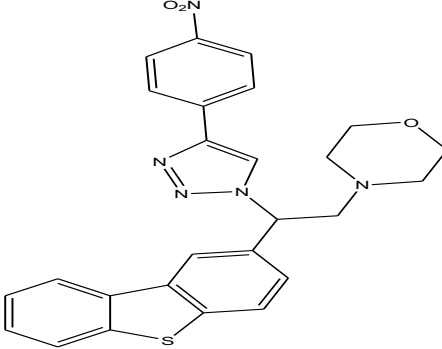
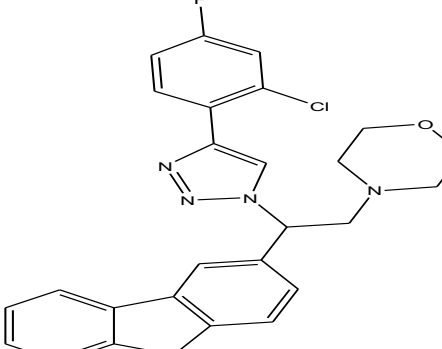
Shastri <i>et al.</i>	Journal of Drug Discovery and Therapeutics (JDDT)				
32		4.3501	4.4743	4.859	6.5207
33		4.3520	4.4804	4.182	2.8665
34		4.3474	4.4771	4.624	1.5708
35		4.3503	4.4781	4.378	5.4090
36		4.3459	4.4740	4.876	5.8507
37	 <p data-bbox="836 1774 917 1816">R=CH</p>	4.3541	4.4793	4.745	2.9364

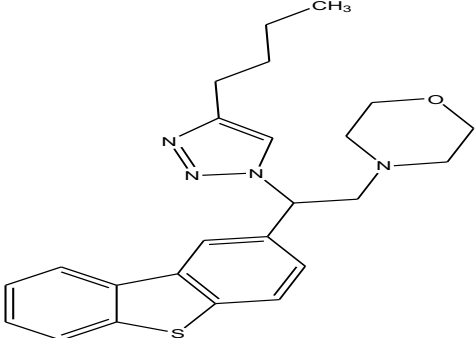
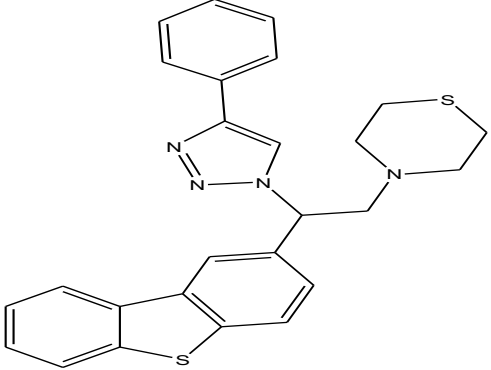
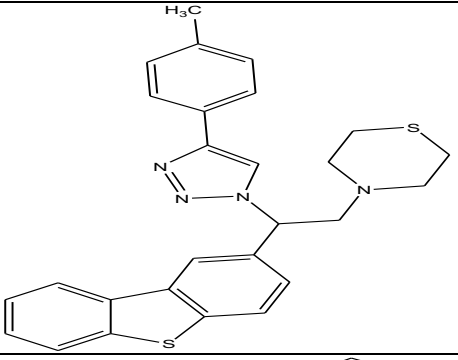
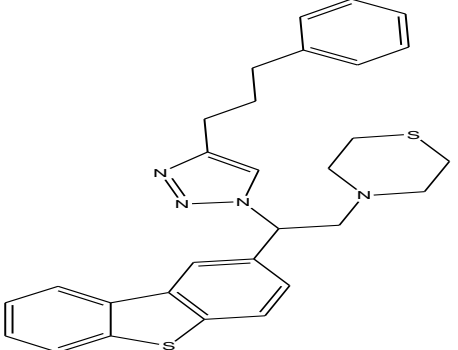
38		4.3471	4.4747	4.796	6.6970
39		4.3451	4.4759	5.016	3.3043
40		4.3460	4.4796	4.654	3.7888
41		4.3508	4.4800	4.947	5.4434
42		4.3467	4.4778	4.883	5.0204
43		4.3460	4.4735	4.876	2.9344
44		4.3436	4.4780	4.596	5.1306

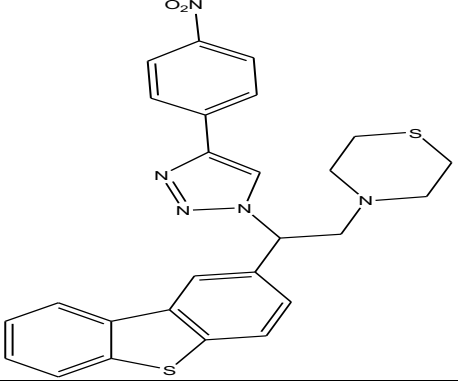
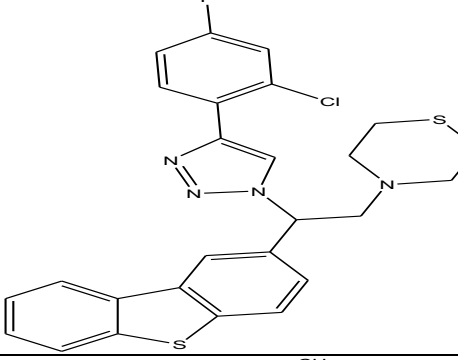
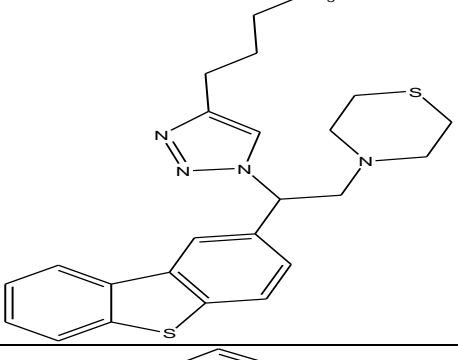
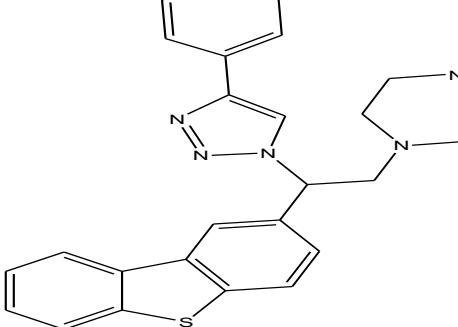
Shastri <i>et al.</i>	Journal of Drug Discovery and Therapeutics (JDDT)				
45		4.3466	4.4739	4.721	7.1182
46		4.3453	4.4722	4.774	5.8317
47		4.3496	4.4784	4.341	4.7399
48		4.3457	4.4786	4.138	6.8212
49		4.3492	4.4780	4.884	8.3985
50		4.3506	4.4769	4.617	8.8636

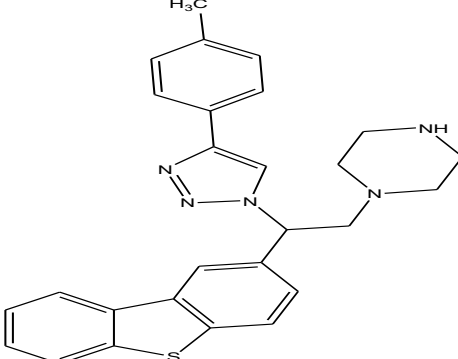
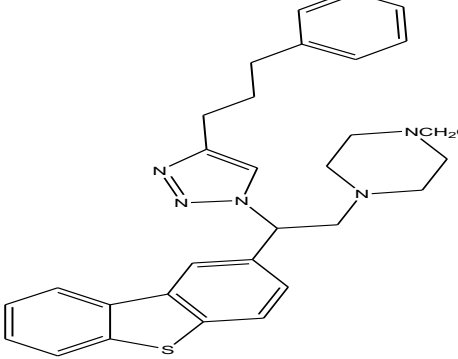
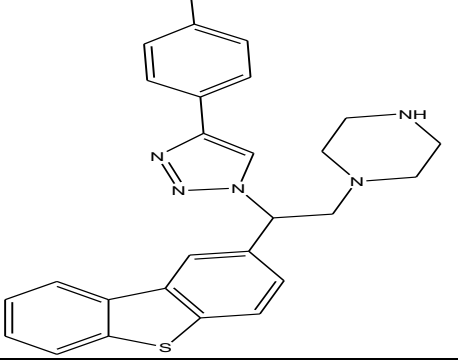
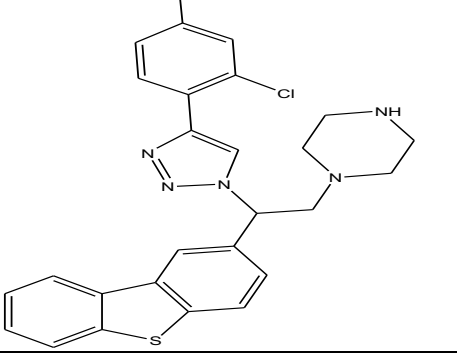
51		4.3534	4.4794	4.872	5.3914
52		4.3452	4.4825	4.118	4.6358
53		4.3407	4.4767	4.721	4.1250
54		4.3337	4.4715	4.019	4.3931

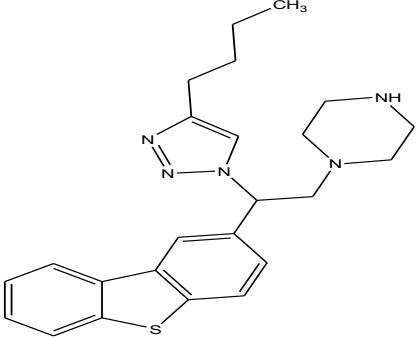
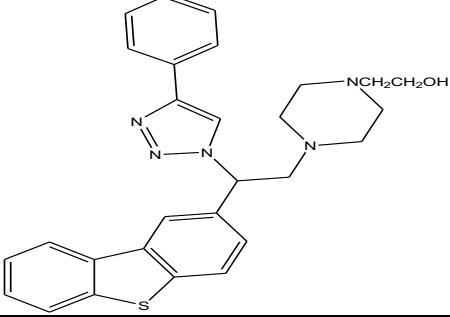
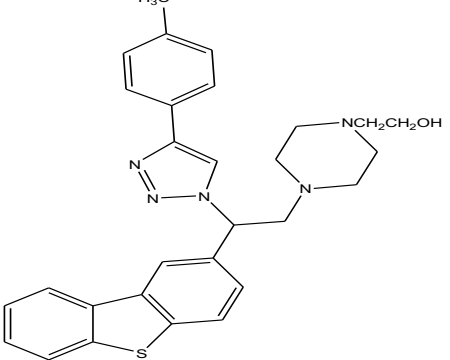
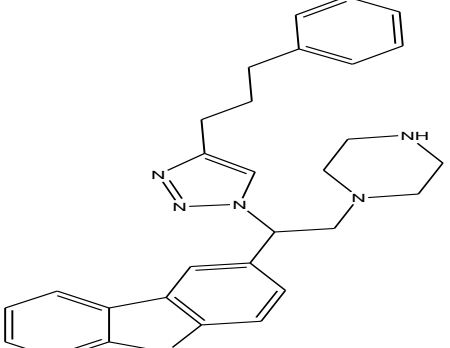
55		4.3493	4.4810	3.527	4.3762
56		4.3333	4.4741	4.387	3.6550
57		4.3369	4.4748	4.606	3.5770
58		4.3357	4.4788	4.269	4.6806

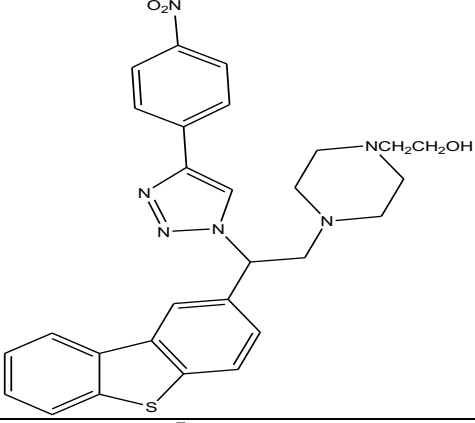
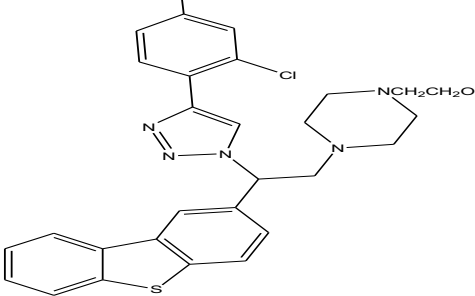
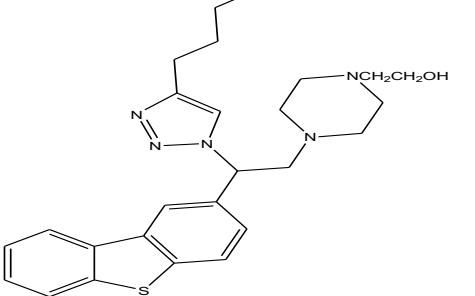
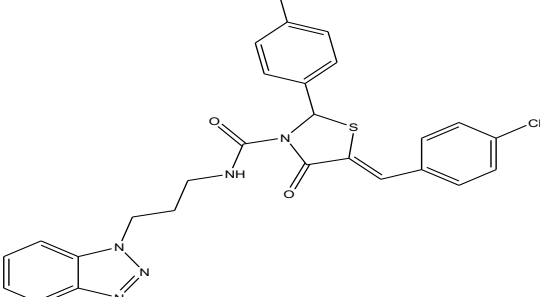
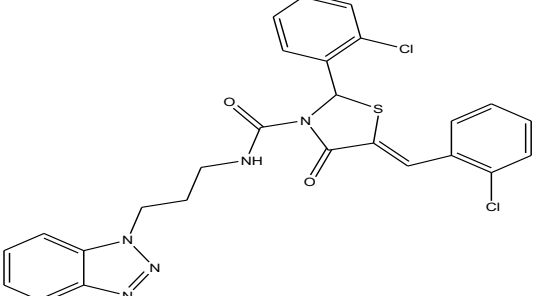
59		4.3387	4.4799	4.137	5.0128
60		4.3391	4.4841	4.116	3.0643
61		4.3340	4.4757	4.447	3.5384
62		4.3432	4.4760	4.193	4.3641

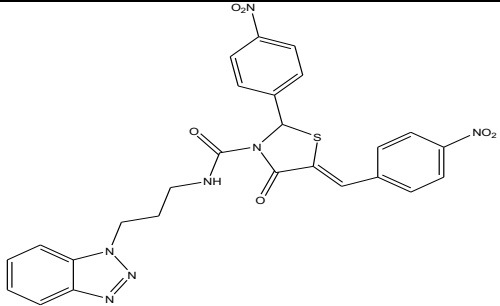
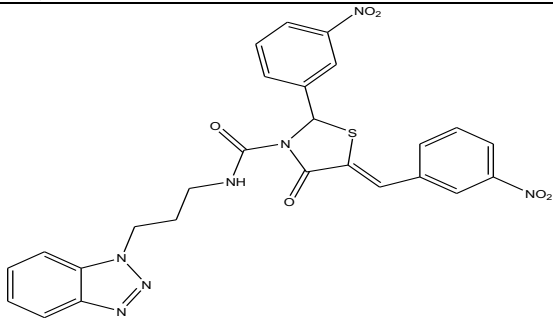
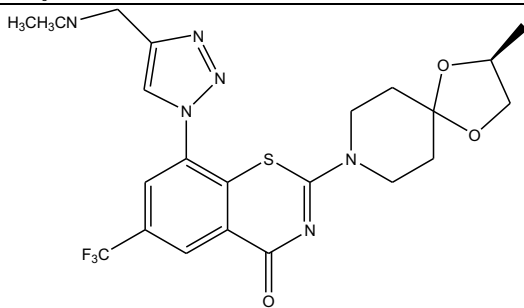
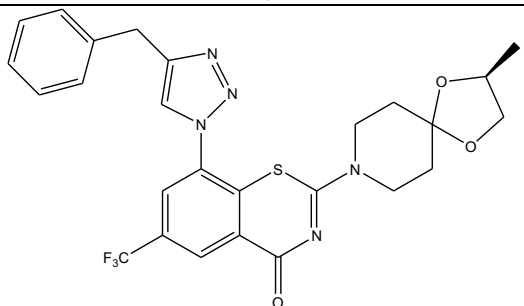
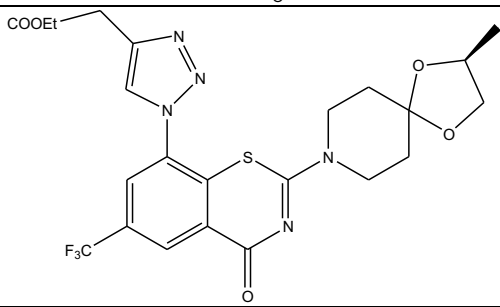
63		4.3346	4.4790	4.208	6.7577
64		4.3416	4.4826	4.032	7.5076
65		4.3332	4.4758	4.285	4.7628
66		4.3472	4.5061	4.814	6.6691

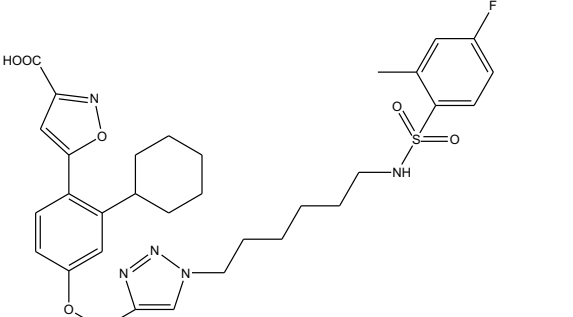
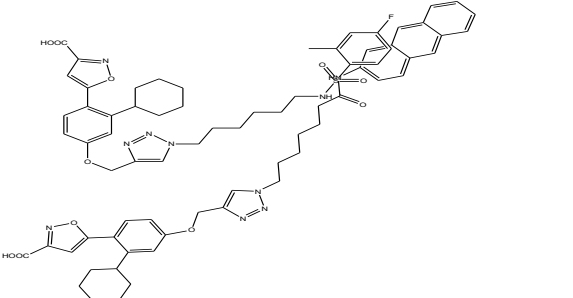
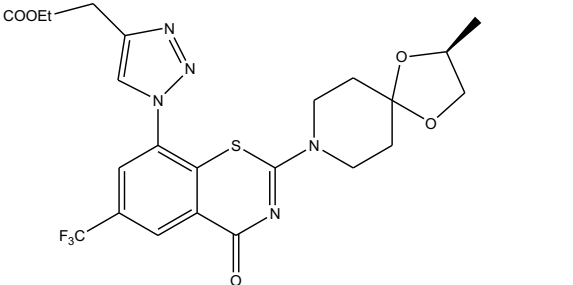
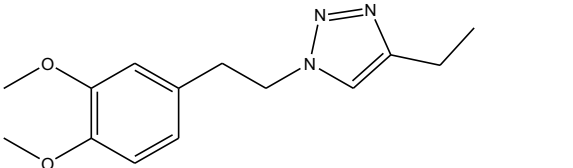
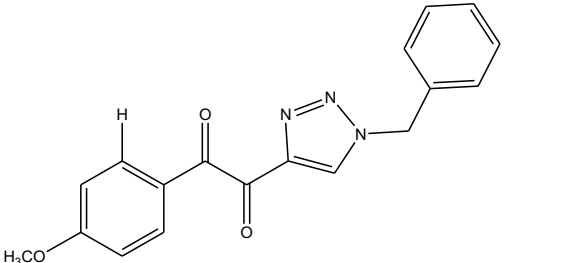
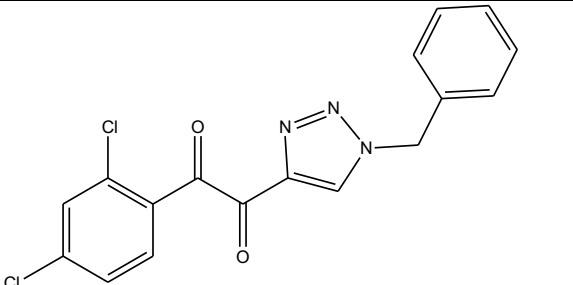
67		4.3332	4.4738	4.288	3.4100
68		4.3387	4.4736	4.415	4.0352
69		4.3325	4.4794	4.382	4.4156
70		4.3435	4.4735	4.514	3.2028

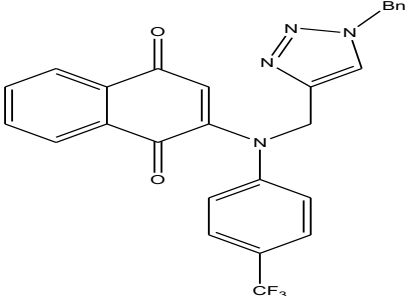
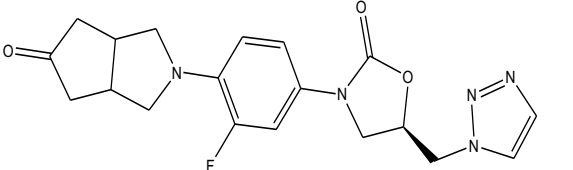
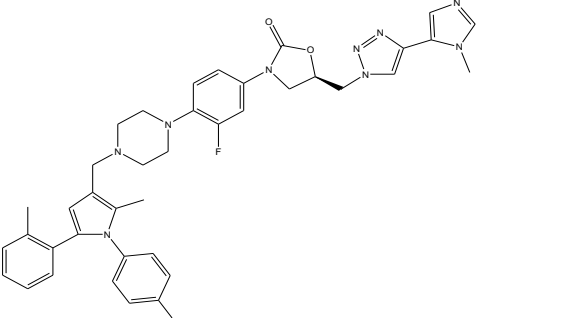
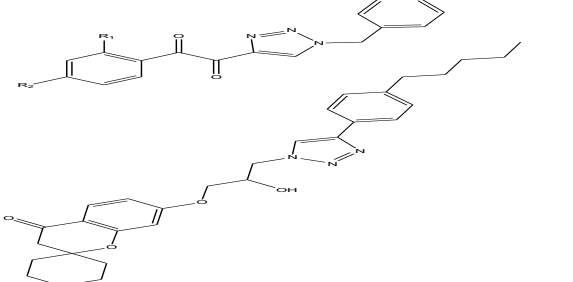
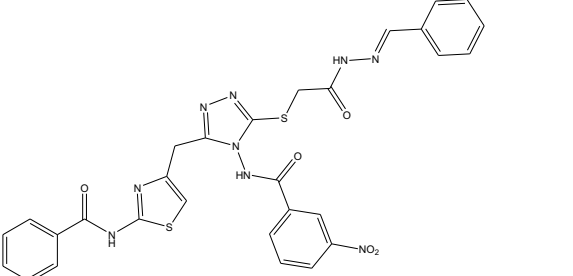
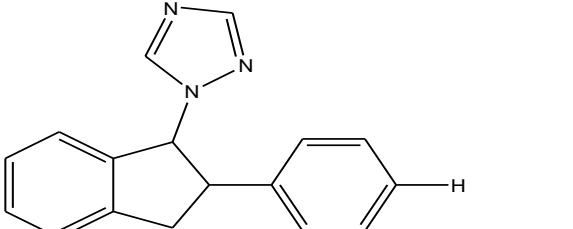
71		4.3430	4.4741	4.631	2.4690
72		4.3355	4.4757	4.338	4.2828
73		4.3354	4.4790	4.208	5.7021
74		4.3320	4.4763	4.556	5.7749

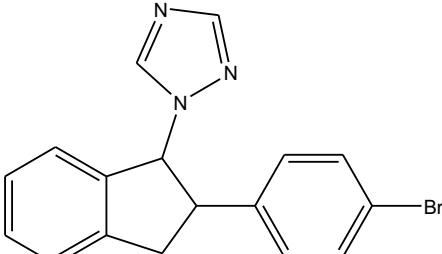
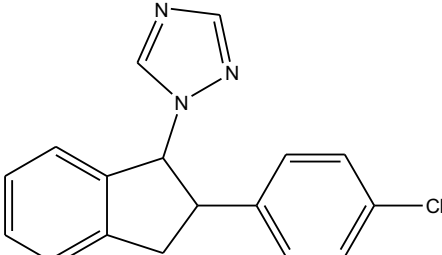
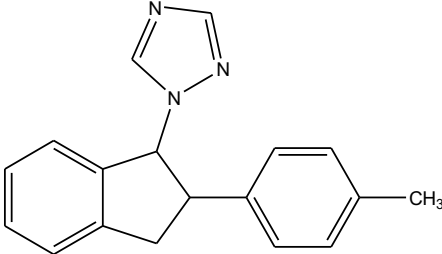
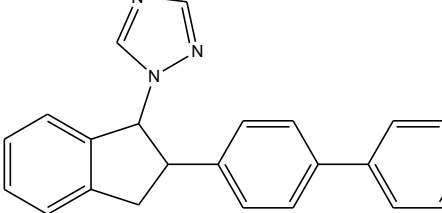
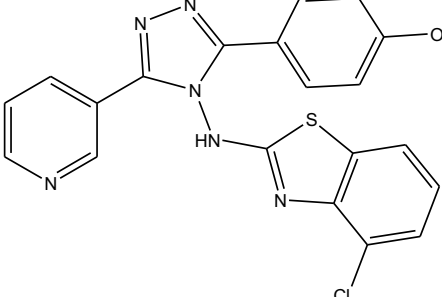
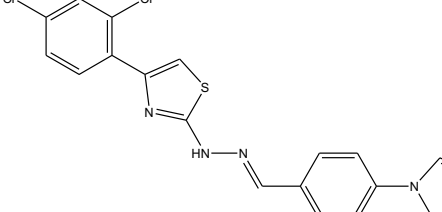
75		4.3352	4.4732	4.517	5.6609
76		4.3348	4.4773	4.433	4.9471
77		4.3306	4.4757	4.575	4.3661
78		4.3350	4.4759	4.428	6.7494

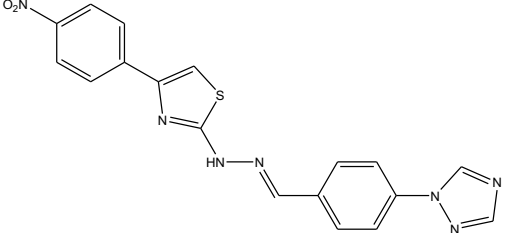
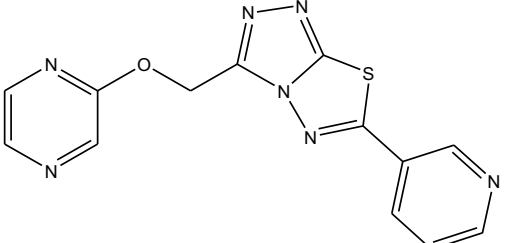
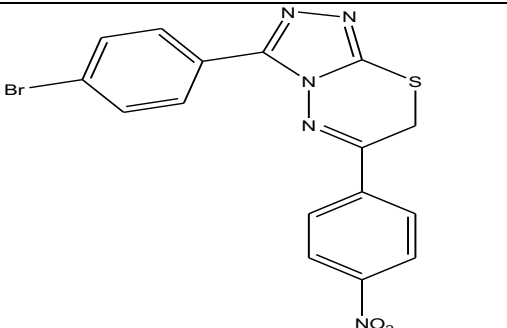
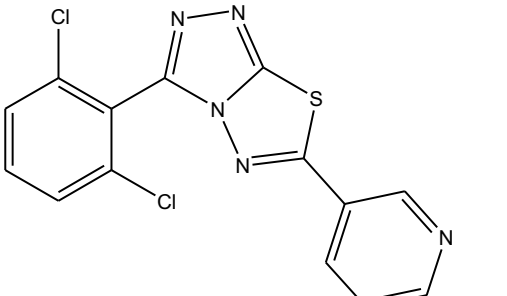
79		4.3378	4.4788	3.984	7.9638
80		4.3361	4.4719	4.629	7.1254
81		4.3276	4.4733	4.466	8.7375
82		4.3353	4.4772	4.246	7.0280
83		4.3350	4.4776	4.55	6.0740

Shastri <i>et al.</i>	Journal of Drug Discovery and Therapeutics (JDDT)				
84		4.3416	4.4835	3.873	4.5000
85		4.3405	4.4790	4.315	3.5902
86		4.3422	4.4739	4.069	5.7215
87		4.3419	4.4705	4.567	5.3869
88		4.3496	4.4736	4.436	3.5564

Shastri <i>et al.</i>	Journal of Drug Discovery and Therapeutics (JDDT)				
89		4.3365	4.4738	4.487	4.6473
90		4.3331	4.4768	4.707	4.2689
91		4.3382	4.4187	4.467	2.5494
92		4.3362	4.4771	4.638	6.4184
93		4.3367	4.4758	4.574	5.6047
94		4.3361	4.4733	4.567	5.1769

Shastri <i>et al.</i>	Journal of Drug Discovery and Therapeutics (JDDT)				
95		4.3407	4.4840	4.287	3.3925
96		4.3322	4.4787	4.412	6.3533
97		4.3330	4.4742	4.465	4.6248
98		4.3389	4.4815	4.032	6.7279
99		4.3357	4.4810	3.828	5.6288
100		4.3427	4.4730	4.575	6.8900

Shastri <i>et al.</i>	Journal of Drug Discovery and Therapeutics (JDDT)				
101		4.3413	4.4776	4.308	7.0763
102		4.3509	4.4830	4.563	3.4315
103		4.5241	4.1082	4.465	3.5404
104		4.3542	4.4651	4.638	6.6284
105		4.6365	4.4742	4.542	5.6307
106		4.3382	4.4187	4.467	2.5444

107		4.6262	4.4701	4.645	6.4544
108		4.5477	4.4958	4.530	5.5230
109		4.5651	4.4745	4.677	5.1745
110		4.3580	4.4654	4.547	2.5365

3. RESULT AND DISCUSION

3.1 CoMFA and CoMSIA Results

To evaluate the quantitative structure–activity relationship (QSAR) of triazole derivatives as α -oxidoreductase inhibitors, 3D-QSAR studies using CoMFA and CoMSIA models were performed.

3.2 CoMFA Analysis

CoMFA models were developed based on various charge calculation methods. Among these, the MMFF94 charge model (Model 6) yielded the best statistical performance. The optimized CoMFA model, constructed using 45 molecules with pIC_{50} values ranging from

3.4661 to 5.2749, showed a cross-validated correlation coefficient $q^2=0.787$, suggesting the model's robustness. The non-cross-validated correlation coefficient was $r^2=0.819$, with a low standard error of estimation (SEE = 0.041), an F-value of 1316.074, and a high predictive correlation coefficient $r^2_{pred}=0.996$, indicating high reliability and predictive power. Steric and electrostatic field contributions were nearly equal, at 0.507 and 0.493 respectively.

Further analysis incorporating additional descriptors such as clogP, CMR, CPSA, and molecular properties under MMFF94 charge conditions provided consistent models, with Model 7 demonstrating strong statistical parameters. The residual values between experimental and predicted pIC₅₀ values for training and test compounds using this model are presented in Table 1. The correlation between actual and predicted pIC₅₀ values is visualized.

3.3 CoMSIA Analysis

CoMSIA models were constructed using different field combinations including steric (S), electrostatic (E), hydrophobic (H), hydrogen

bond donor (D), and acceptor (A). The model incorporating all five fields (Model 28) exhibited the best results, with $q^2=0.805$, $r^2=0.831$, $r^2_{pred}=0.831$, $SEE = 0.065$, $F\text{-value} = 520.302$, and $r^2_{pred}=0.990$. The field contributions were: steric (0.151), electrostatic (0.268), hydrophobic (0.223), donor (0.234), and acceptor (0.124). Model 29 (MMFF94) emerged as the optimal CoMSIA model using the most appropriate combination of field descriptors. The actual vs. predicted pIC₅₀ values and residuals for this model.

Table 2 Residual values of Training set and Test set of molecules of the CoMFA model 7.

S No.	IC ₅₀	pIC ₅₀	Predicted pIC ₅₀	Residual Value
1*	112.40	3.6579	3.8016	-0.1437
2	42.26	4.3639	3.8789	0.485
3	202.16	3.6213	3.8078	-0.1865
4*	303.52	3.4117	4.0432	-0.6315
5	204.44	3.6873	3.8829	-0.1956
6	174.21	3.7563	3.9741	-0.2178
7	35.75	4.4347	3.8897	0.545
8*	16.23	4.7392	4.0403	0.6989
9	64.52	4.1642	3.9498	0.2144
10	323.91	3.4661	3.9013	-0.4352
11	145.40	3.7534	3.9112	-0.1578
12*	364.41	3.3722	3.7974	-0.4252
13	181.70	3.7173	3.8383	-0.121
14	142.81	3.8362	3.8785	-0.0423
15	193.55	3.7132	3.8534	-0.1402
16*	99.16	4.0037	4.016	-0.0123
17	123.32	3.909	3.9062	0.0028
18	55.43	4.2563	3.8841	0.3722
19	226.32	3.6453	3.8988	-0.2535
20	175.72	3.7552	3.9677	-0.2125
21	46.39	4.3336	4.0258	0.3078
22	6.50	5.1871	4.9646	0.2225
23	10.23	4.9901	4.9235	0.0666
24	11.29	4.9473	5.0454	-0.0981
25	8.48	5.0716	4.9601	0.1115
26	11.22	4.95	5.0041	-0.0541

27	6.97	5.1568	5.027	0.1298
28	5.55	5.2557	5.0047	0.251
29*	12.75	4.8945	4.9155	-0.021
30	15.09	4.8213	4.9923	-0.171
31	5.58	5.2534	5.0292	0.2242
32*	26.38	4.5787	4.983	-0.4043
33	7.12	5.1475	4.9941	0.1534
34	16.17	4.7913	5.0014	-0.2101
35	8.05	5.0942	5.0036	0.0906
36*	28.02	4.5525	4.9661	-0.4136
37	18.33	4.7368	5.0323	-0.2955
38	8.37	5.0773	5.0028	0.0745
39	8.07	5.0931	4.9718	0.1213
40	5.31	5.2749	4.968	0.3069
41	11.09	4.9551	4.9889	-0.0338
42	9.12	5.0357	4.9485	0.0872
43	53.34	4.2729	5.0297	-0.7568
44*	44.8	4.3487	4.9767	-0.628
45	11.85	4.9263	5.0492	-0.1229

Table 3: CoMSIA on training set at different charges at MMFF94 charge

Sno	Name	q ²	r ²	SE	NC
1	Model 24 S	0.784	0.813	0.266	1
2	Model 25 SE	0.794	0.825	0.258	1
3	Model 26 SHE	0.805	0.832	0.252	1
4	Model 27 SEHD	0.803	0.830	0.254	1
5	Model 28 SEHDA	0.805	0.831	0.253	1

Table 4: CoMSIA with MMFF94 Charge

Sno	Model	q ²	r ²	SE	NC
1	Model 29 clogP	0.800	0.854	0.239	2
2	Model 30 CMR	0.793	0.845	0.247	2
3	Model 31 CPSA	0.792	0.838	0.252	2
4	Model 32 DM	0.779	0.855	0.238	2
5	Model 33 MP Area	0.791	0.843	0.248	2
6	Model 34 MP PSA	0.800	0.846	0.245	2
7	Model 35 MP PV	0.794	0.844	0.247	2
8	Model 36 MP Vol	0.790	0.845	0.247	2
9	Model 37 Mol-Wt	0.795	0.848	0.244	2
10	Model 38 Atom Count	0.788	0.844	0.247	2
11	Model 39 Bond Count	0.792	0.843	0.248	2
12	Model 40 Chiral	0.805	0.831	0.253	1
13	Model 41 Ring Count	0.796	0.853	0.240	2
14	Model 42 RotBonds	0.783	0.848	0.244	2

3.4 CoMFA and CoMSIA Contour Map Analysis

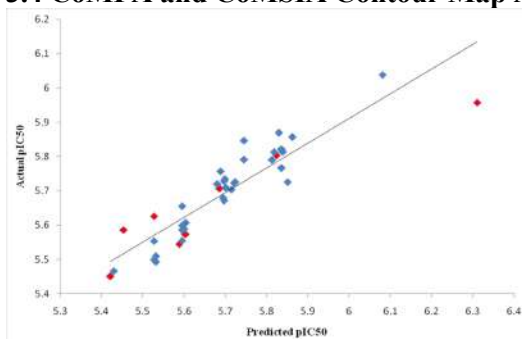


Figure 1: Graph of actual versus predicted pIC₅₀ values of the training set and the test set molecules of Model 7 (MMFF94) using the CoMFA model.

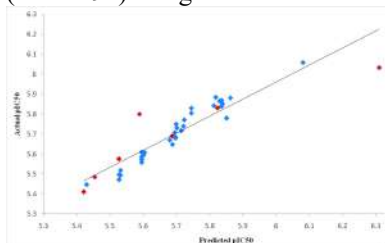


Figure 2: Graph of actual versus predicted pIC₅₀ values of the training set and the test set molecules of Model 29 (MMFF94) using the CoMSIA model.

3.5 CoMFA Contour Maps

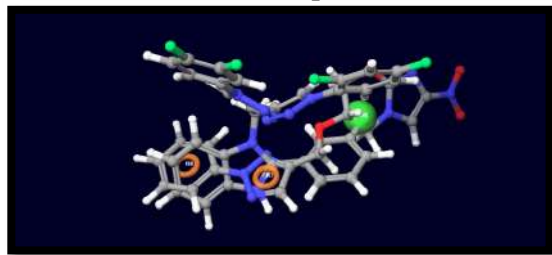


Figure 2: Contour map of Compound 36

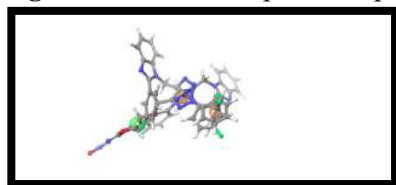


Figure 3: Contour map of Compound 13.



3.6: Reference compound 13 with contour for designing.

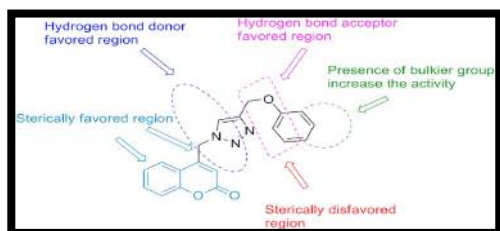


Figure 4: Std* coeff contour maps of CoMSIA analysis with 2Å grid spacing in combination with compound 36 and 13. 5.4.1 – 5.4.10 shows Steric, electrostatic, hydrophobic, acceptor and donor.

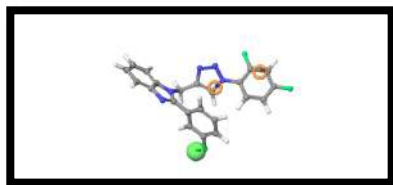
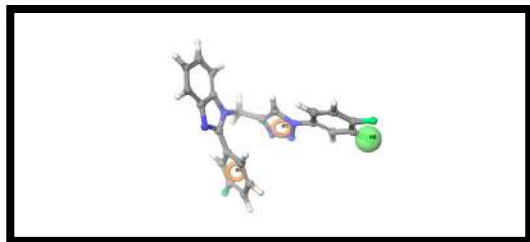


Figure 5 and 6: Contour map of Compound 36 and 13 Steric:

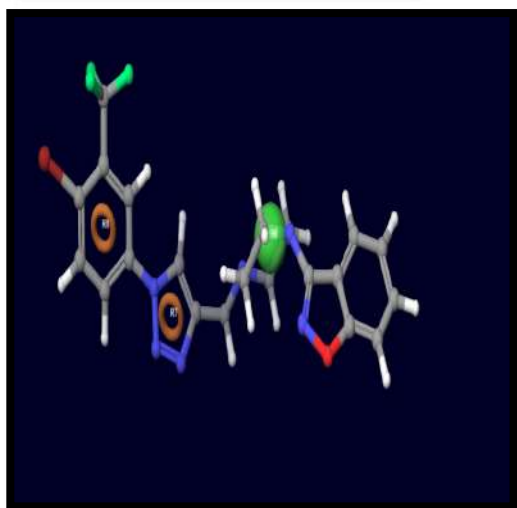
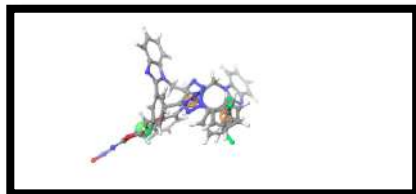


Figure 7 and 8: Contour map of Compound 36 and 13 electrostatic:

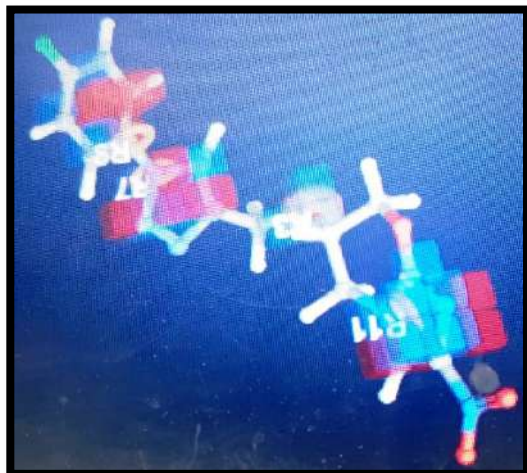


Figure 9: Contour map of Compound 36 hydrophobic:

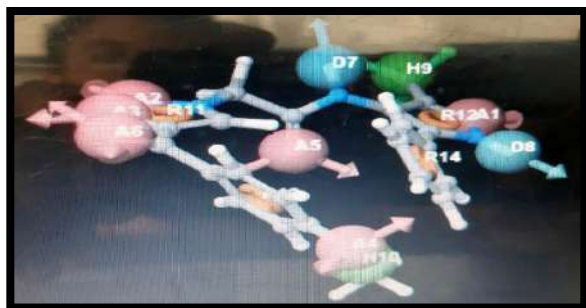
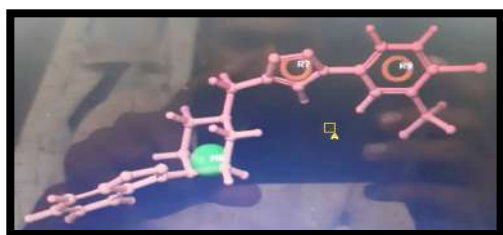


Figure 10 and 11: Contour map of Compound 36 and 13 donor:

CoMFA contour maps were generated to interpret the influence of steric and electrostatic fields on biological activity. Compounds 28 and 40 were selected as reference structures. Green contours indicate regions where bulky groups enhance activity, observed at the 1st, 7th, and 8th positions of the benzoimidazole ring and phenyl rings. Yellow contours near the 5th and 6th positions of the imidazole ring and adjacent phenyl rings suggest steric hindrance is unfavorable.

Electrostatic contours show blue regions—favorable for electron-donating groups—at the imidazole and phenyl ring positions. Red contours, indicating preference for electron-

withdrawing groups, were observed on the C=O group attached to the phenyl ring.

3.7 CoMSIA Contour Maps

The best CoMSIA model was visualized through contour maps using compounds 36 and 13 as references:

- **Steric Fields:** Green contours on phenyl rings and azo groups indicate favorable sites for bulky groups. Yellow contours around the 5th and 6th positions of the imidazole ring suggest bulky substitutions here are detrimental.
- **Electrostatic Fields:** Blue contours on the R₁ phenol ring and aldehyde group denote beneficial electron-donating

substitutions. Red contours on nitrogen-attached aldehyde and phenol rings indicate favorable electron-withdrawing groups.

- **Hydrophobic Fields:** Yellow contours indicate regions where hydrophobic groups enhance activity, such as on the R₁ phenol ring and imidazole-attached benzene. White contours denote non-favorable hydrophobic regions.
- **Acceptor Fields:** Magenta contours show where hydrogen bond acceptor groups are favorable—particularly around nitrogen linkages—while red contours mark regions where such groups are not desirable.
- **Donor Fields:** Cyan contours near aldehyde-related nitrogen show favorable hydrogen donor sites, whereas purple

contours on central benzene rings indicate unfavorable regions for donor groups.

3.8 HQSAR Results

Hologram QSAR (HQSAR) models were developed for a dataset of 46 compounds (37 training, 9 test). The best model demonstrated excellent internal and external validation with $q^2=0.800$, $q^2 = 0.800$, $q^2=0.800$ and $r^2=0.943$, $r^2=0.943$. The most predictive model employed fragment distinction parameters A/B/C/Ch and fragment size 2–6 with a hologram length of 151 and six optimum components.

Further statistical enhancements were achieved by varying fragment size and distinction combinations. These results underline HQSAR's strong predictive capability and its utility in rational anti-diabetic drug design.

Table 5: The determination of statistical parameters for the models of the series based on different distinct with default size 4-7.

Sno	Fragment Distinct	q^2	r^2	q^2 SE	r^2 SE	Ensemble	Best length	NC
1	A/B	0.792	0.946	0.286	0.150	0.948	151	6
2	A/B/H	0.771	0.955	0.300	0.141	0.939	353	6
3	A/B/C	0.800	0.943	0.276	0.160	0.933	257	6
4	A/B/Ch	0.787	0.951	0.290	0.147	0.947	151	6
5	A/B/C/H	0.794	0.950	0.285	0.149	0.937	151	6
6	A/B/DA	0.797	0.941	0.278	0.163	0.937	257	6
7	A/B/C/DA	0.781	0.947	0.289	0.154	0.935	353	6
8	A/B/C/Ch	0.800	0.943	0.276	0.160	0.933	257	6
9	A/B/H/DA	0.793	0.932	0.285	0.174	0.922	257	6
10	A/B/H/Ch	0.785	0.939	0.291	0.164	0.930	257	6
11	A/B/Ch/DA	0.796	0.937	0.276	0.168	0.933	353	6
12	A/B/C/H/DA	0.773	0.961	0.298	0.132	0.946	353	6
13	A/C/H/DA	0.783	0.951	0.292	0.148	0.939	257	6
14	A/C/H/Ch/DA	0.782	0.944	0.293	0.158	0.935	307	6

Table 6: For Test:

Pred R ²	SE	Bond Length	NC
0.938	0.166	307	6

Table 7: The determination of statistical parameters for the model of the series based on different fragment size fragment distinct A/B/C.

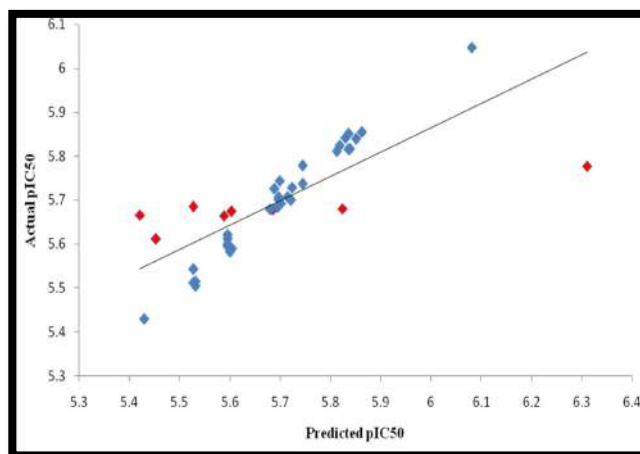
S no	Name	q ²	r ²	q ² SE	r ² SE	Ensemble	Best length	NC
1	2-5	0.800	0.907	0.276	0.204	0.903	97	6
2	3-6	0.800	0.921	0.277	0.188	0.917	307	6
3	4-7	0.800	0.943	0.250	0.160	0.933	257	6
4	5-8	0.785	0.953	0.286	0.144	0.945	307	6
5	6-9	0.786	0.952	0.290	0.146	0.946	151	6
6	7-10	0.781	0.957	0.293	0.138	0.951	257	6
7	8-11	0.779	0.959	0.299	0.135	0.956	307	6
8	2-6	0.801	0.920	0.276	0.189	0.917	151	6
9	3-7	0.799	0.951	0.277	0.148	0.933	257	6
10	4-8	0.787	0.951	0.289	0.148	0.942	151	6
11	5-9	0.791	0.949	0.291	0.151	0.944	353	6
12	6-10	0.785	0.954	0.246	0.143	0.947	257	6

Table 8: Residual value of molecules of the HQSAR model

S. No.	Actual	Predicted pIC50	Residual	Sno.	Actual	Predicted pIC50	Residual
1*	3.6579	3.84	-0.1821	24	4.9473	5.03886	-0.09156
2	4.3639	4.31899	0.04491	25	5.0716	5.18102	-0.10942
3	3.6213	3.70718	-0.08588	26	4.95	4.98164	-0.03164
4*	3.4117	3.897	-0.4853	27	5.1568	5.05202	0.10478
5	3.6873	3.65625	0.03105	28	5.2557	5.17937	0.07633
6	3.7563	3.72401	0.03229	29*	4.8945	5.034	-0.1395
7	4.4347	4.40343	0.03357	30	4.8213	4.82304	-0.00174
8*	4.7392	3.581	1.1582	31	5.2534	5.17144	0.08196
9	4.1642	3.97353	0.19067	32*	4.5787	4.882	-0.3033
10	3.4661	3.85838	-0.39228	33	5.1475	5.02115	0.12635
11	3.7534	3.68661	0.06679	34	4.7913	4.63785	0.15345
12*	3.3722	4.281	-0.9088	35	5.0942	5.05461	0.03959
13	3.7173	3.60906	0.10824	36*	4.5525	5.275	-0.7225
14	3.8362	3.78962	0.04658	37	4.7368	4.9274	-0.1906
15	3.7132	3.85739	-0.14419	38	5.0773	5.31175	-0.23445
16*	4.0037	4.665	-0.6613	39	5.0931	5.13309	-0.03999
17	3.909	3.93422	-0.02522	40	5.2749	4.91999	0.35491
18	4.2563	4.10691	0.14939	41	4.9551	4.85028	0.10482
19	3.6453	3.99175	-0.34645	42	5.0357	4.96971	0.06599
20	3.7552	3.81998	-0.06478	43	4.2729	4.65657	-0.38367
21	4.3336	3.97848	0.35512	44	4.3487	4.588	-0.2393
22	5.1871	4.98552	0.20158	45	4.9263	5.10494	-0.17864
23	4.9901	5.09693	-0.10683	46	4.9539	4.89264	0.06126

Table 9: Summary of the statistical parameters of HQSAR studies:

S. No	Statistical parameters	Model (A/B/C)	Model (A/B/C/Ch)
1	Fragment size	2-6	2-6
2	q^2	0.801	0.801
3	r^2	0.920	0.920
4	Ensemble	0917	0.917
5	SE	0.189	0.189
6	NC	6	6
7	Best Length	151	151

**Figure 12:** Graph of actual versus predicted pIC₅₀ values of the training set and the test set molecules of Model A/B/C at 2-6 fragment size using the HQSAR.**3.9 Interpretation of HQSAR contours:**

The contribution map obtained from the HQSAR module implemented in SYBYL-X 2.0 uses colour schemes to discriminate individual atomic contribution to activity. The colour encoded in structure fragment at the red end of the spectrum (red, red-orange, orange) reflect poor contribution, whereas colours encoded in structure fragments at the green end (yellow, green-blue and green) reflects favourable contribution. Atoms with the intermediate or moderate contribution on pharmacological activity are coloured as white. The intermediate contributor was helpful in maintaining the common structure was helpful in maintaining the common structure only but they are not contributing more towards the activity. Compound 40 and 28 are selected and their contour obtained. A green colour at the 2nd and 4th position of imidazole ring, yellow colour at the 3rd position, blue-green colour at the N atom of the thiazole ring and benzene ring attached to it, and nitrogen-nitrogen bond attached next to

aldehyde group are required for the enhanced activity.

White colour of the on the Sulphur atom of thiazole ring and phenol ring at R₁ position shows intermediate activity. The contour of compounds 40 and 28 are given in figure 5.4.6. One more molecule named compound 43 was taken as it is showing some negative contribution with red colour on the benzene ring attached at the R₁ position and the orange colour on the nitrogen-nitrogen bond attached to the aldehyde shown.

3.10: Pharmacophore Modelling:

Ten GALAHAD models were generated by using training set compounds. Model 8 and 10 had high energy which is considered to be due to steric clashes, leading to their exclusion from the analysis. The other 20 models were generated and evaluated successively by the test database constructed previously. Table shows the predictable results for each model. Model 8 with the highest value was considered to be the best model.

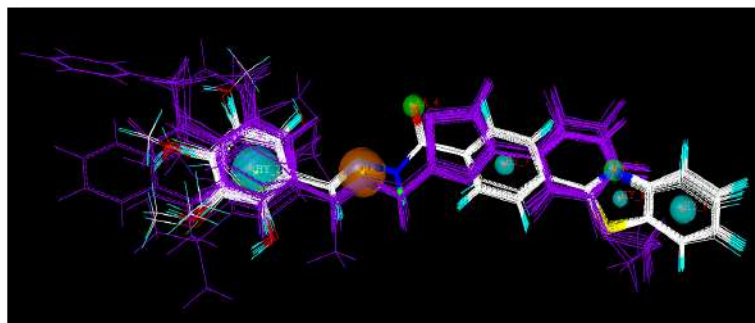


Figure 13: Pharmacophore model 8 and molecular alignment of the compound

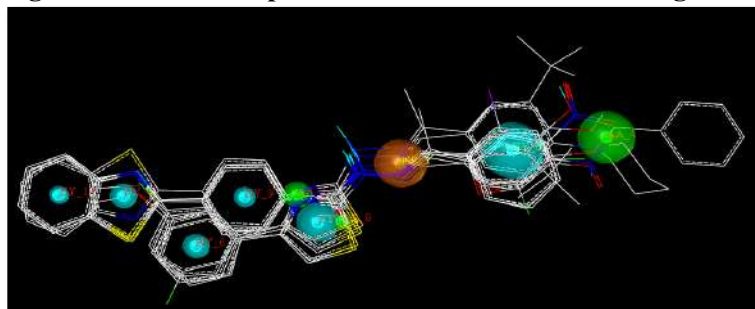


Figure 14: Alignment of all test set compounds using pharmacophore modelling.

Table 10: The parameter values of Training set for each pharmacophore model:

NAME	Specific.	N HITS	FEATS	PARETO	Energy	Steric	HBOND	MOL_QRY
Model_001	3.818	-16	8	0	12.16	1344.7	328.5	102.39
Model_002	3.651	-16	9	0	11.05	1302.6	326.7	101.73
Model_003	3.812	-16	8	0	15.43	1431.7	326.1	103.38
Model_004	1.66	-16	9	0	8.05	1217.9	321.6	104.1
Model_005	3.823	-16	8	0	10.95	1338.4	320.8	104.34
Model_006	4.979	-16	8	0	17.59	1255.7	336	107.9
Model_007	3.814	-16	8	0	15.09	1308.6	325	107.49
Model_008	3.822	-16	8	0	10.95	1292.2	326.7	72.97
Model_009	3.8	-16	9	0	9.89	1340.7	322.1	66.9
Model_010	3.825	-16	8	0	8.36	1159.2	326.5	88.92

Table 11: The parameter value of Test set for each pharmacophore model:

NAME	Specific.	N_HITS	FEATS	PARETO	Energ.	Steric	HBOND	MOL_QRY
Model_001	3.710	0	14	0	7.91	1363.50	279.80	119.80
Model_002	3.774	2	13	0	11.75	1144.60	287.40	119.56
Model_003	3.391	9	12	0	11.12	1394.50	250.20	96.99
Model_004	3.405	8	12	0	12.78	1487.70	277.80	90.49
Model_005	3.710	0	14	0	15.08	1232.30	286.00	107.41
Model_006	3.767	1	13	0	21.92	1191.60	287.80	112.80
Model_007	3.398	9	12	0	14.83	1035.00	288.10	112.07
Model_008	3.477	9	11	0	11.15	1288.20	281.60	58.79
Model_009	2.399	9	12	0	16.15	1233.70	282.00	95.57
Model_010	2.371	9	13	0	180.71	1170.10	292.10	97.11

3.11: Pharmacophore mapping interpretation:

The pharmacophore features of Model 8, where cyan colour on the imidazole ring, a phenolic ring attached to it and the phenolic ring attached to the azo group showed the hydrophobes, green colour on the nitrogen atom of imidazole ring and the double bond O attached to the phenolic ring showed the HB acceptors and magenta colour on the azo group shows the HB donor.

The Model 8 includes seven pharmacophore features: four hydrophobes, two HB acceptors and one HB donor.

3.12: Docking Analysis:

All compounds of training set and test set were selected for docking analysis in order to evaluate their oxidoreductase inhibitor activity. For the

docking analysis PDB selected was 5JFO. Using Schrödinger Maestro version 2016 and 5JFO PDB docking was done and found that all compounds were showing good docking score as shown in table for training set and test set.

PDB descriptions: 1GAH PDB: 5JFO (M. enoyl-reductase InhA in complex with GSK625).

Name of Ligand: ACR

Chemical name of the ligand: N-{1-[(2-chloro-6-fluorophenyl)methyl]-1H-pyrazol-3-yl}-5-[(1S)-1-(3-methyl-1H-pyrazol-1-yl)ethyl]-1,3,4-thiadiazol-2-amine

Chemical Formula : C₂₁H₂₇N₇O₁₄P₂

Structure Ligand:

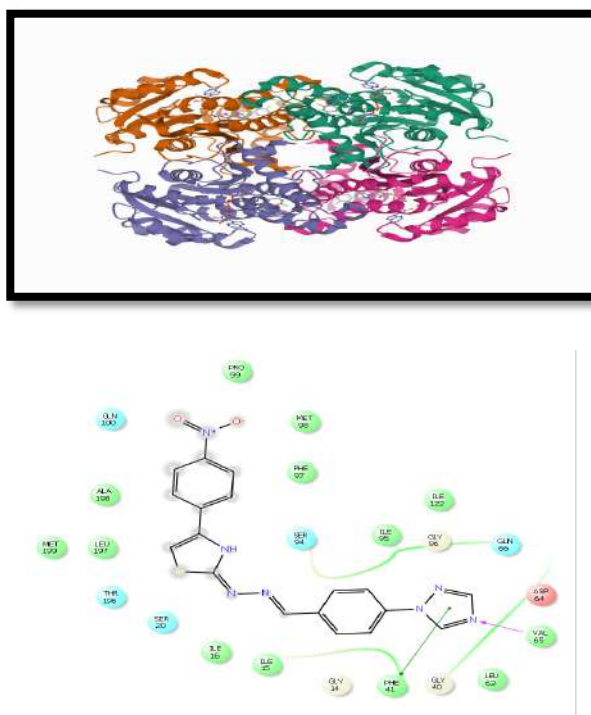


Figure 15 and 16

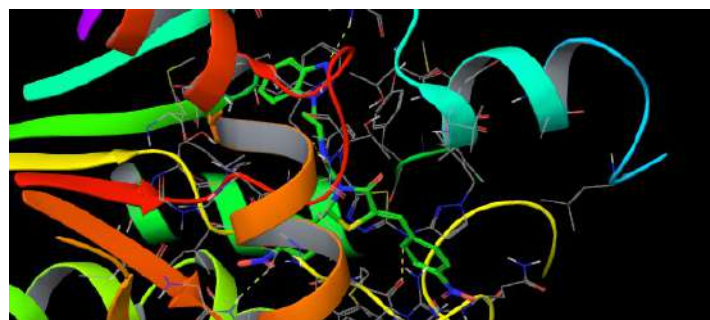
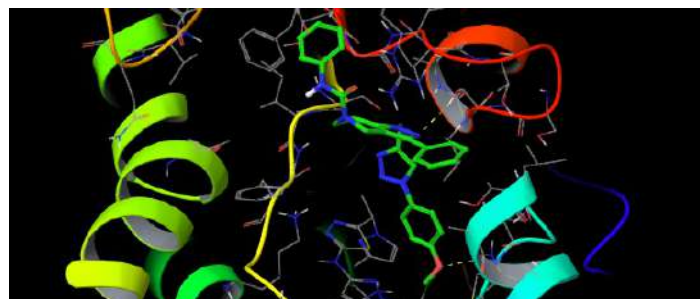
3.13: Results of Docking studies and interaction points of Imidazole derivatives on 5JFO PDB:

Table 11: Docking score of all compounds:

Sno	Compound	Total Score	Sno	Compound	Total Score	Sno.	Compound	Total Score
1	20	8.75	16	28	6.49	31	3	5.33
2	22	8.58	17	27	6.48	32	25	5.18
3	7	7.87	18	11	6.47	33	23	5.03
4	46	7.67	19	13	6.46	34	33	4.93
5	26	7.56	20	17	6.43	35	36	4.89

6	30	7.54	21	10	6.32	36	18	4.88
7	38	7.39	22	19	6.22	37	9	4.84
8	15	7.3	23	16	6.18	38	39	4.81
9	8	7.27	24	4	5.92	39	2	4.75
10	43	7.21	25	12	5.9	40	34	4.33
11	21	7.11	26	29	5.83	41	24	4.04
12	31	7.11	27	5	5.79	42	37	3.89
13	45	7.06	28	14	5.79	43	44	3.69
14	42	6.76	29	35	5.75	44	32	3.44
15	41	6.54	30	6	5.43	45	40	3.24

3.14: Docking pose view of the compound 36 and 13 based on 5JFO PDB:



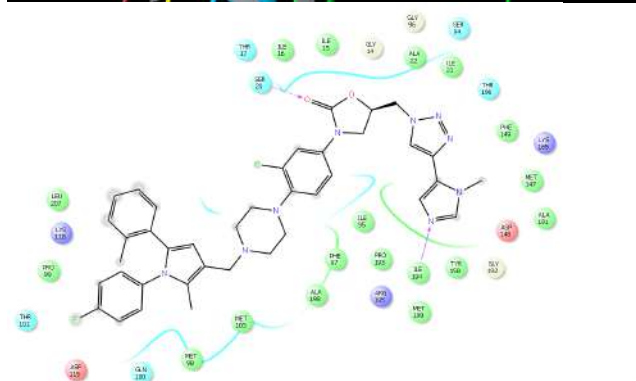
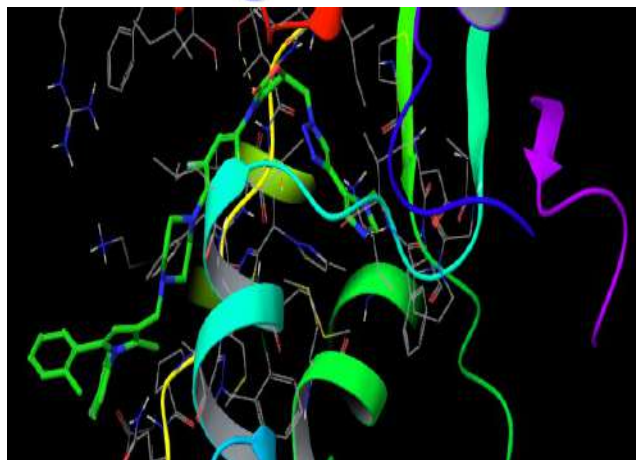
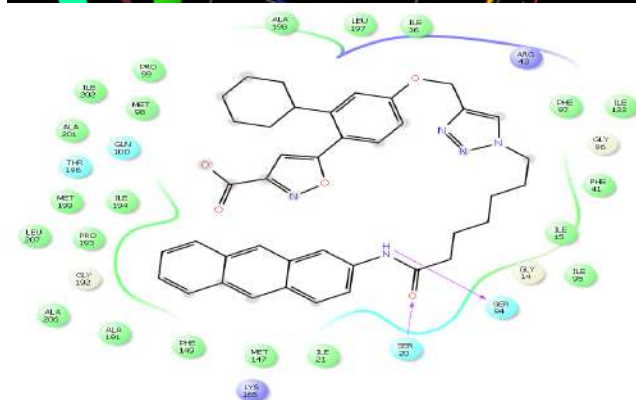
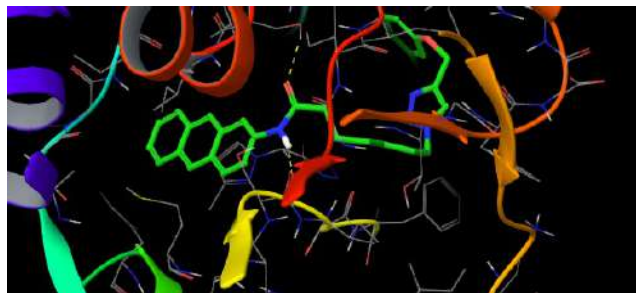




Figure 17, 18, 19, 20, 21 22, 23, 24,25, 26, 27, 28, 29: Full Docking view of all compounds on 5JFO PDB:

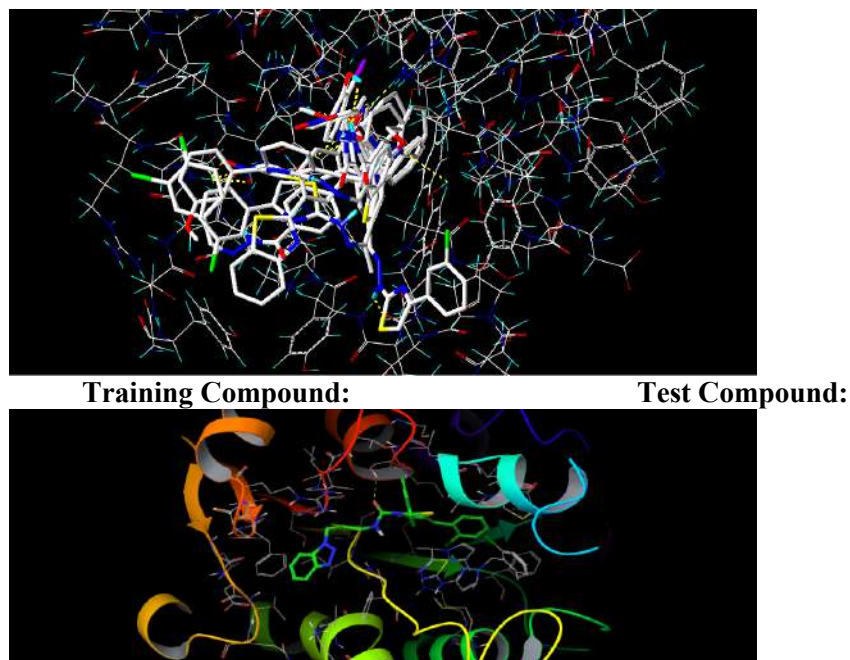


Figure 30 and 31: Interaction point of compound 36:

3.15 Designing of Compounds:

Based on the CoMFA, CoMSIA, HQSAR, Docking and Pharmacophore mapping studies, compound 36 and 13, with the highest activity, was taken as a template to design new compounds.

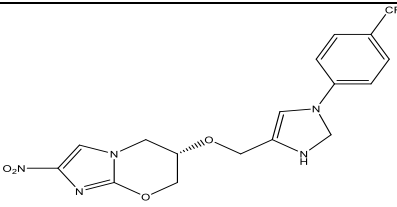
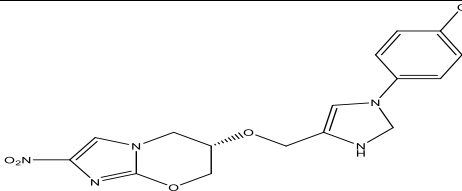
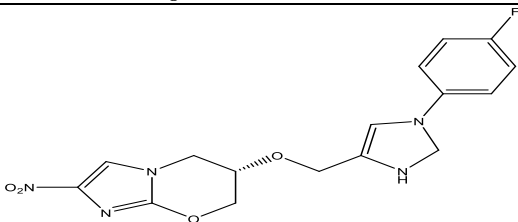
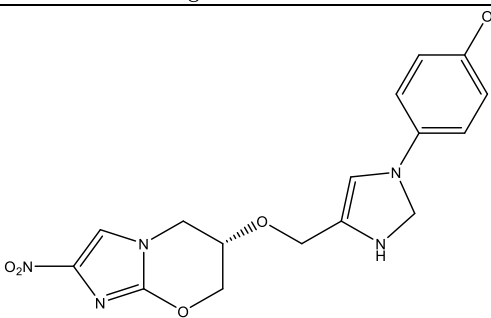
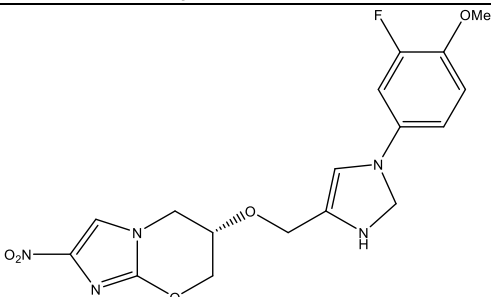
A set of 110 new compounds with approximately similar predicted activity were designed and assessed.

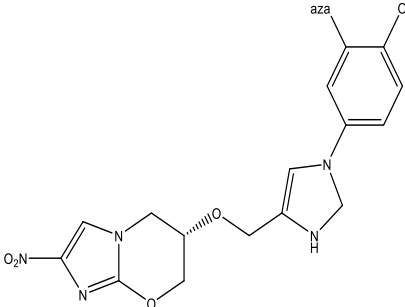
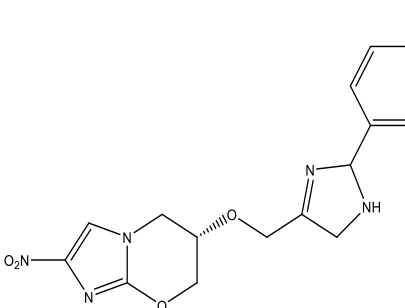
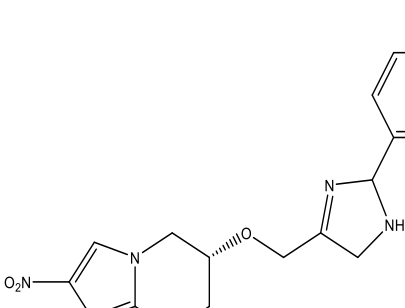
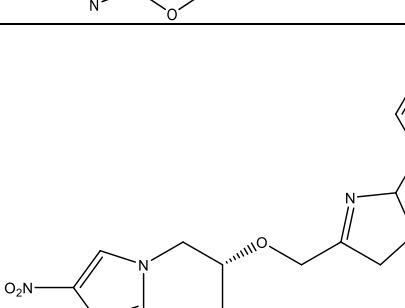
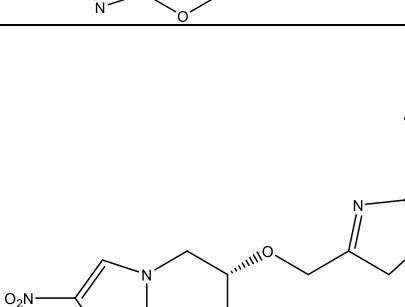
These molecules were aligned to the database and their activities were predicted by the

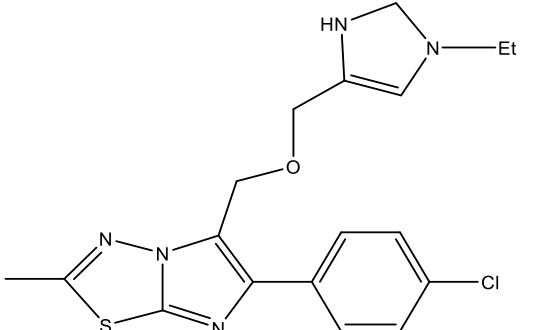
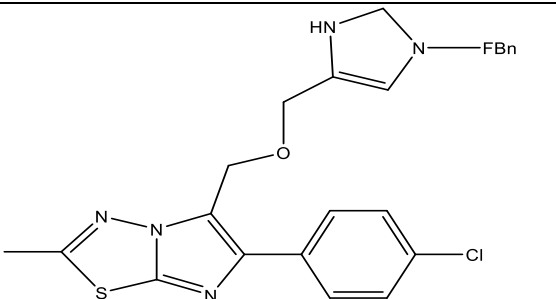
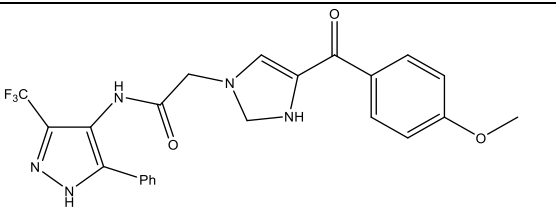
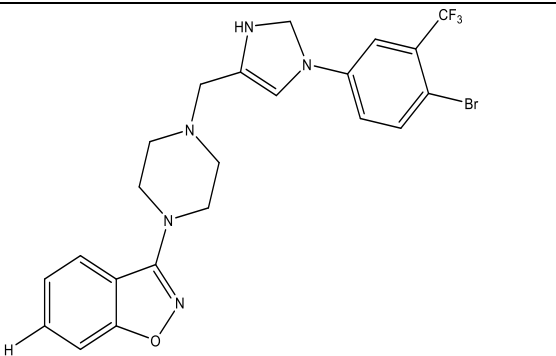
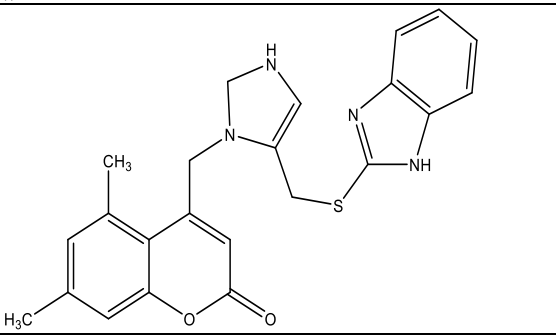
CoMFA, CoMSIA, HQSAR, Docking and Pharmacophore mapping models previously established. The chemical structures and predicted pIC_{50} values of these compounds and the graph of their predicted pIC_{50} values versus the most active compound 40 and 28.

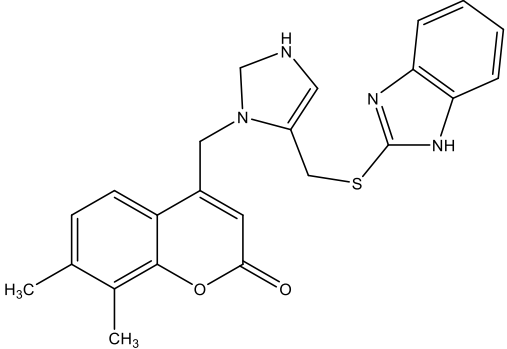
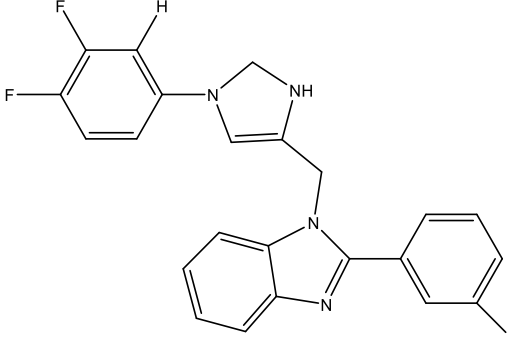
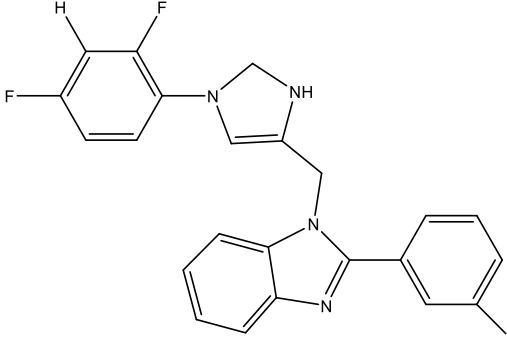
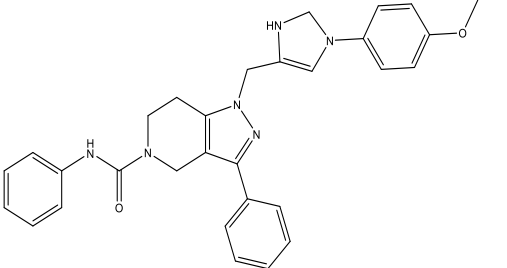
Most of the molecules show significant improved predicted activities but not as much as compared to compound 40 and 28. The results validated the structure activity relationship obtained by this study.

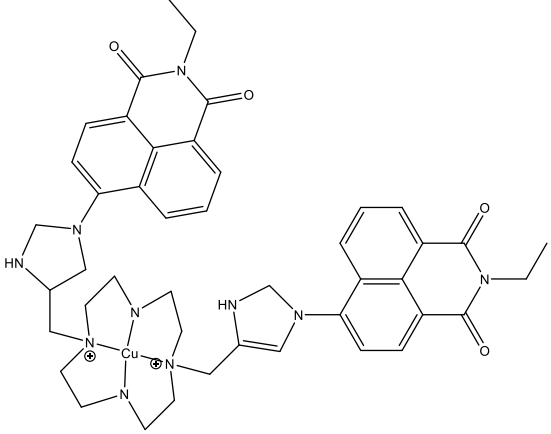
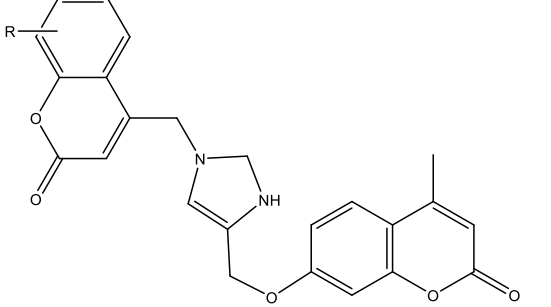
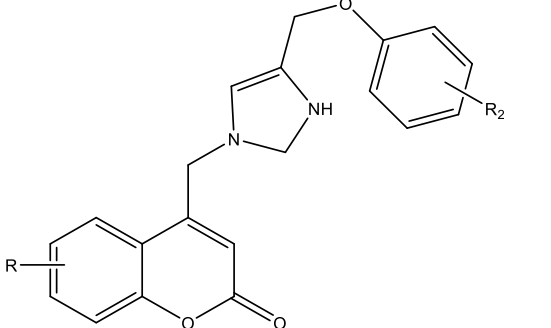
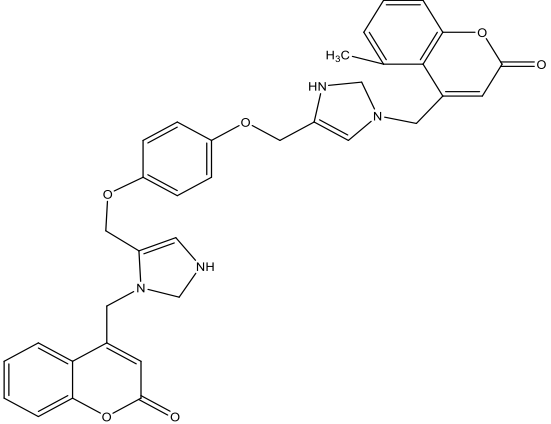
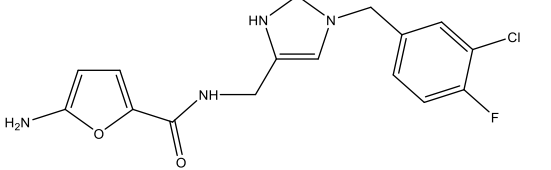
Table 12: The structures and predicted pIC₅₀ values of newly designed derivatives

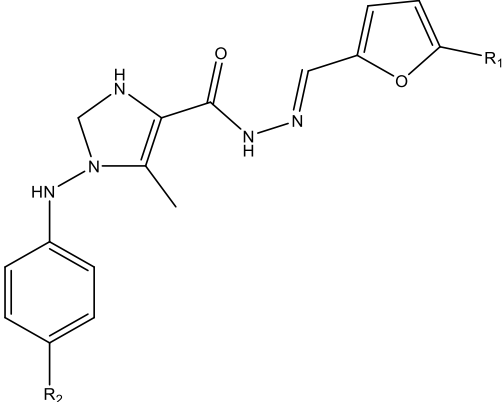
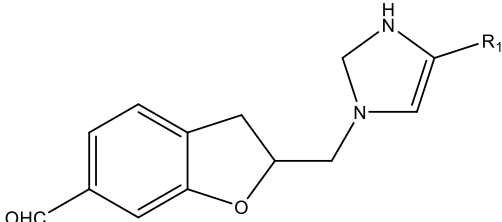
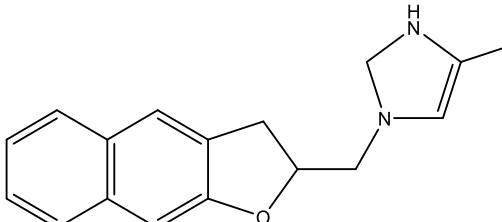
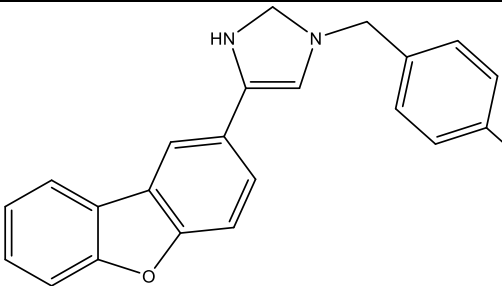
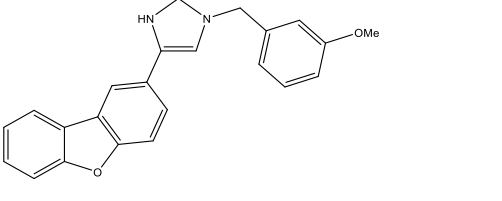
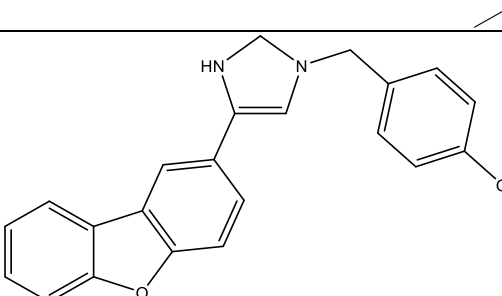
Compound d	Compound structure	Pred pIC ₅₀		HQSA R	Dockin g Score
		CoMF A	CoMSI A		
1	 <p>(S)-2-nitro-6-((1-(4-(trifluoromethyl)phenyl)-2,3-dihydro-1H-imidazol-4-yl)methoxy)-6,7-dihydro-5H-imidazo[2,1-b][1,3]oxazine</p>	4.3521	4.4758	4.282	4.5033
2		4.3484	4.4751	5.03	3.8241
3		4.3438	4.4782	4.328	3.6918
4		4.3534	4.4803	3.836	5.3139
5		4.3477	4.4731	4.696	5.4296

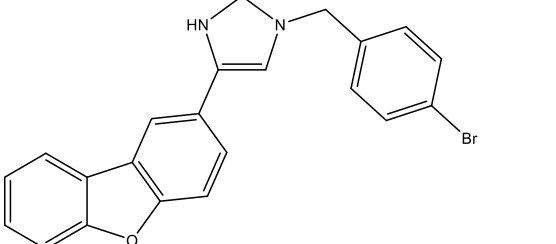
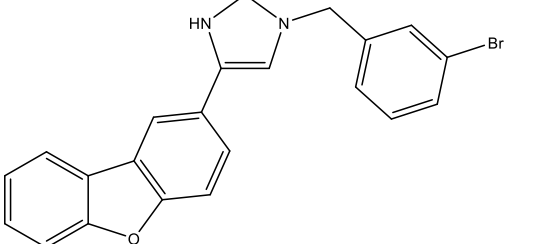
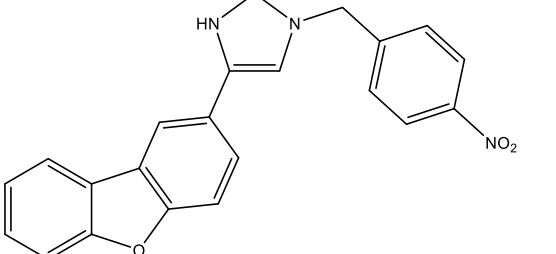
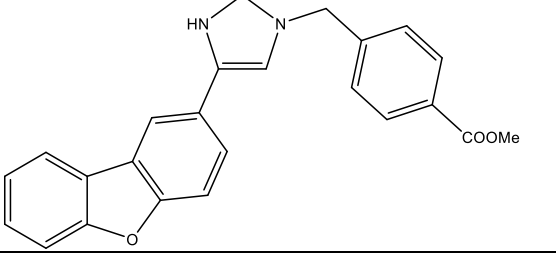
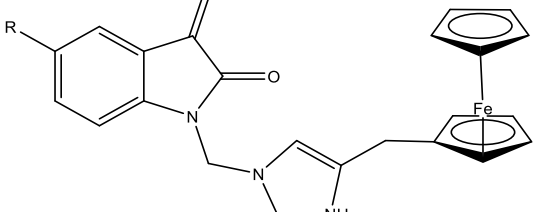
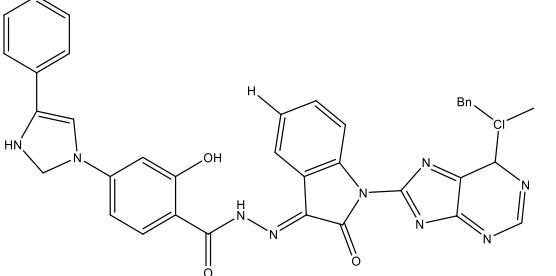
6		4.3456	4.4747	4.915	3.0611
7		4.3488	4.4753	4.578	4.3919
8		4.3493	4.4782	4.447	4.9245
9		4.3486	4.4808	4.425	2.9629
10		4.3502	4.4784	4.756	3.8114

Shastri <i>et al.</i>	Journal of Drug Discovery and Therapeutics (JDDT)				
11		4.3511	4.4776	4.503	2.3645
12		4.3450	4.4755	4.518	5.3367
13		4.3493	4.4778	4.341	5.9438
14		4.3443	4.4748	4.594	4.8035
15		4.3536	4.4984	5.123	6.0693

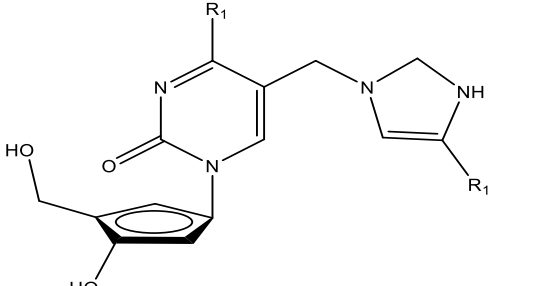
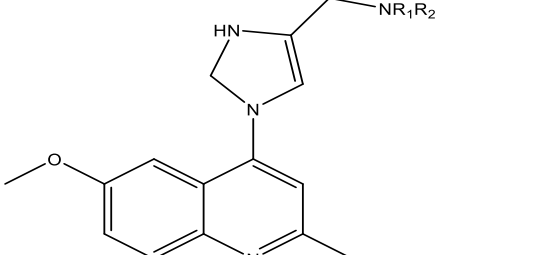
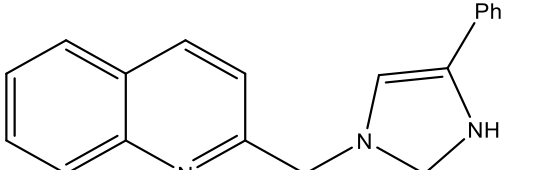
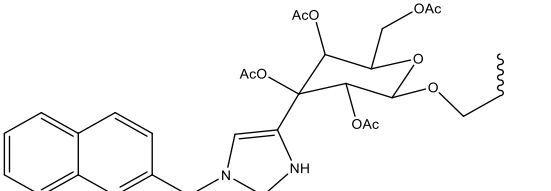
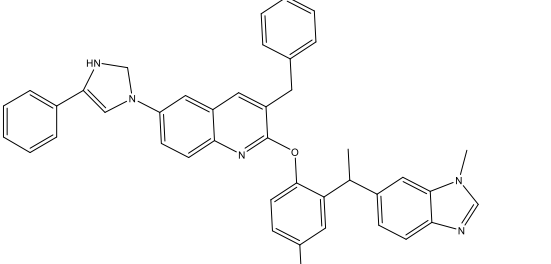
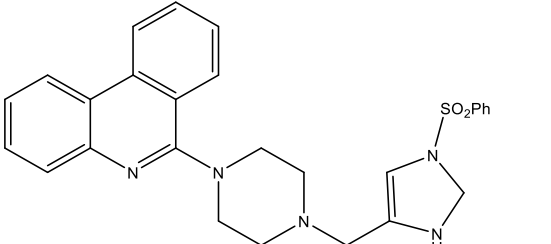
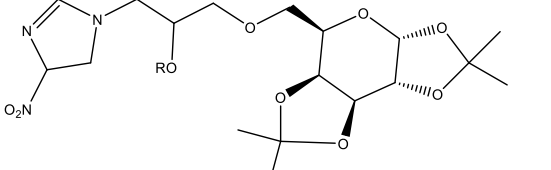
16		4.3456	4.4717	4.597	2.7969
17		4.3462	4.4732	4.725	4.5086
18		4.3469	4.4785	4.691	4.7630
19		4.3495	4.4753	4.823	3.3900

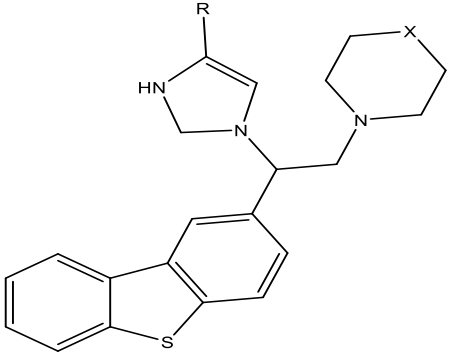
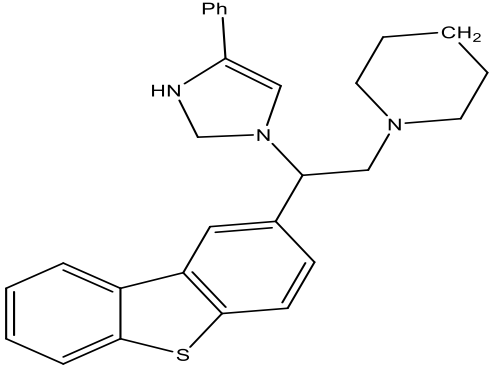
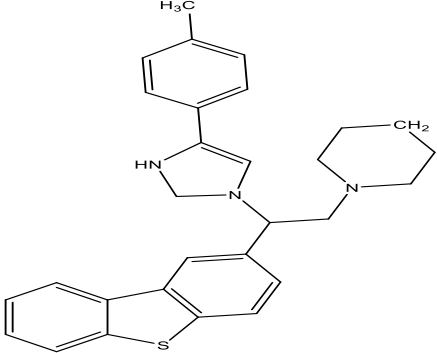
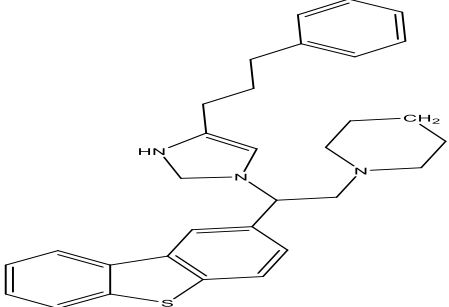
20		4.3480	4.4792	4.941	3.0896
21		4.3461	4.4752	4.647	2.8599
22		4.3492	4.4802	4.518	4.9646
23		4.3465	4.4702	4.866	6.6412
24		4.3452	4.4737	4.826	4.7953

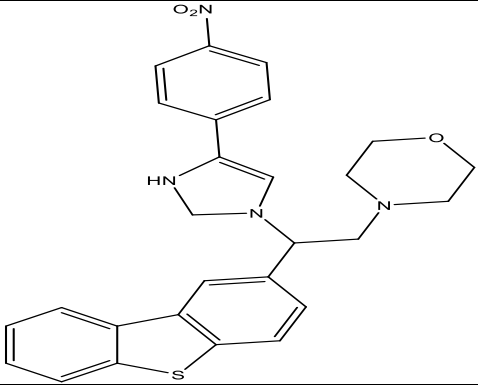
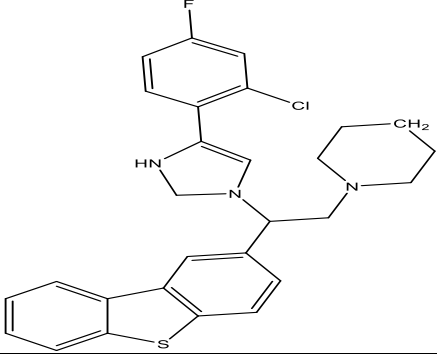
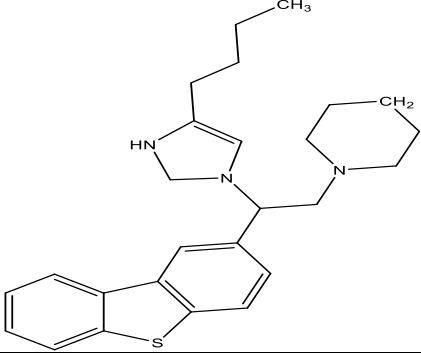
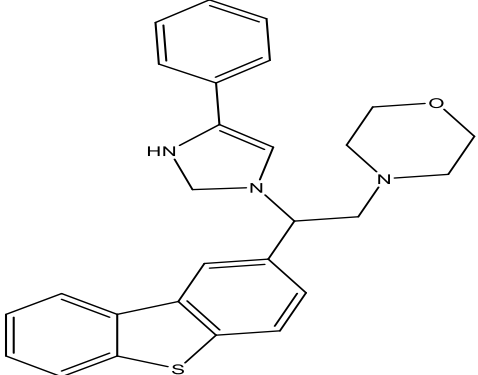
25		4.3467	4.4783	4.742	5.2871
26		4.3453	4.4697	4.884	6.3892
27		4.3514	4.791	4.373	8.2615
28		4.3473	4.4783	4.293	5.4088
29		4.3470	4.4761	4.939	6.3040
30		4.3431	4.4754	4.775	4.8325

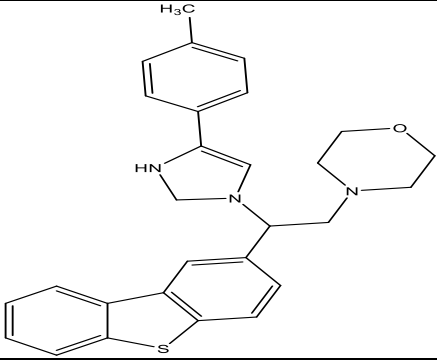
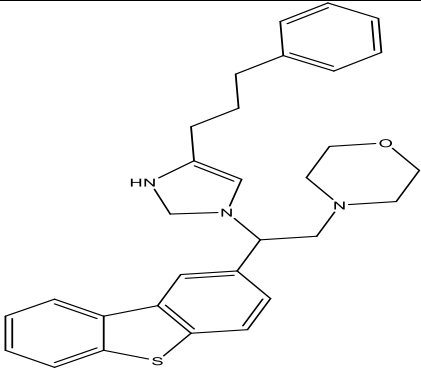
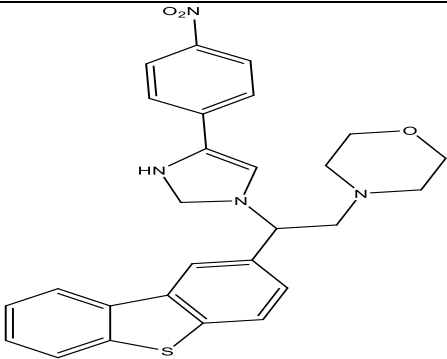
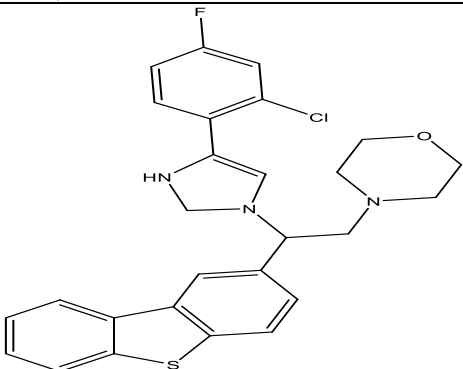
Shastri <i>et al.</i>	Journal of Drug Discovery and Therapeutics (JDDT)				
31		4.3454	4.4758	4.555	4.9260
32		4.3501	4.4743	4.859	6.5207
33		4.3520	4.4804	4.182	2.8665
34		4.3474	4.4771	4.624	1.5708
35		4.3503	4.4781	4.378	5.4090
36		4.3459	4.4740	4.876	5.8507

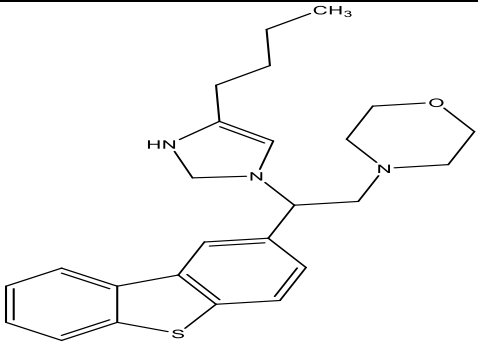
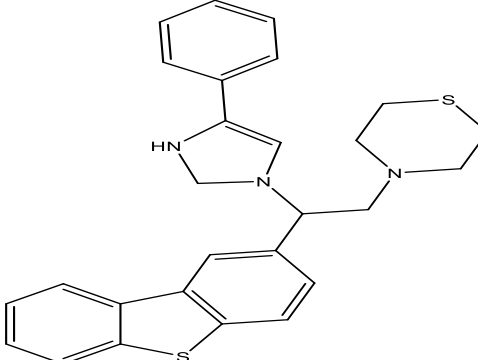
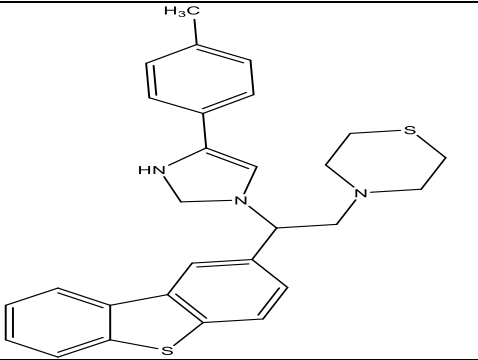
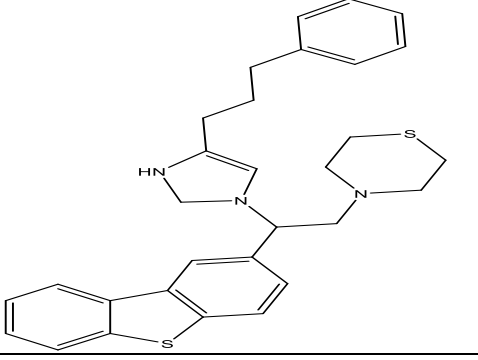
37	 H ₃	4.3541	4.4793	4.745	2.9364
38		4.3471	4.4747	4.796	6.6970
39		4.3451	4.4759	5.016	3.3043
40		4.3460	4.4796	4.654	3.7888
41		4.3508	4.4800	4.947	5.4434
42		4.3467	4.4778	4.883	5.0204
43		4.3460	4.4735	4.876	2.9344

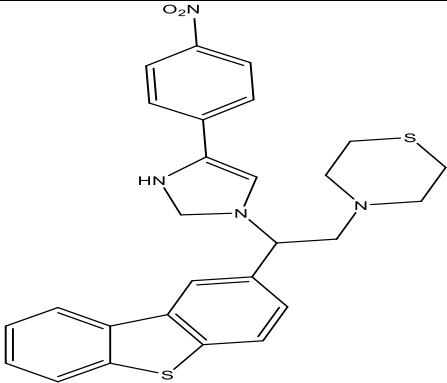
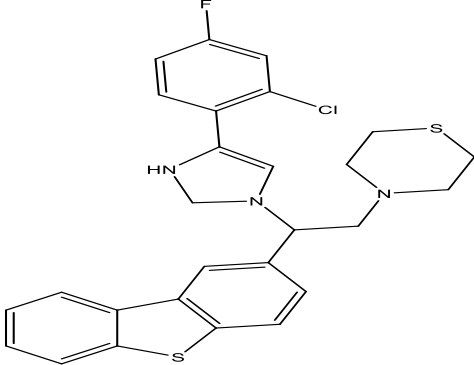
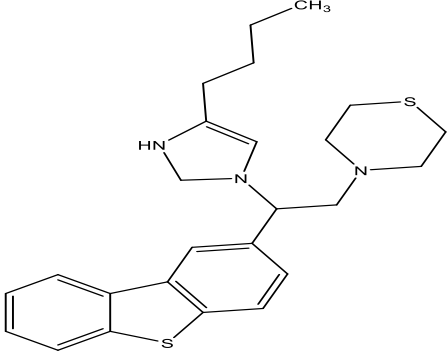
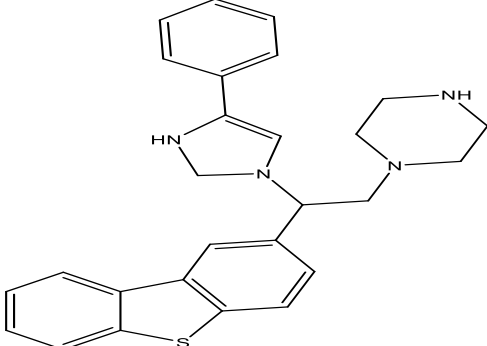
Shastri <i>et al.</i>	Journal of Drug Discovery and Therapeutics (JDDT)				
44		4.3436	4.4780	4.596	5.1306
45		4.3466	4.4739	4.721	7.1182
46		4.3453	4.4722	4.774	5.8317
47		4.3496	4.4784	4.341	4.7399
48		4.3457	4.4786	4.138	6.8212
49		4.3492	4.4780	4.884	8.3985
50		4.3506	4.4769	4.617	8.8636

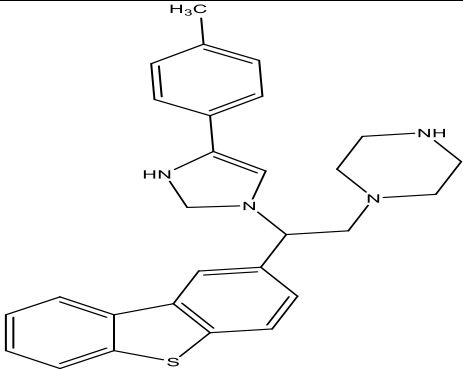
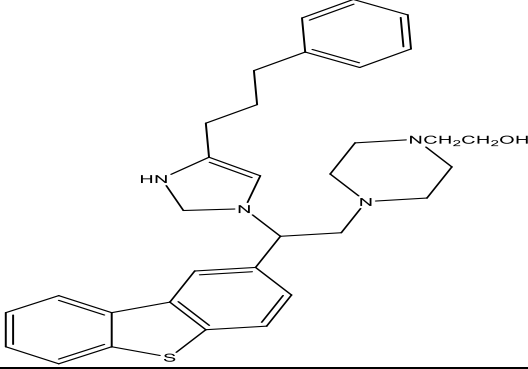
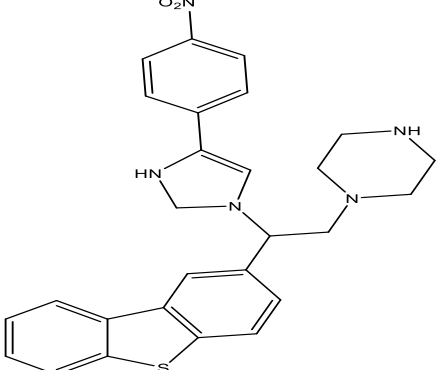
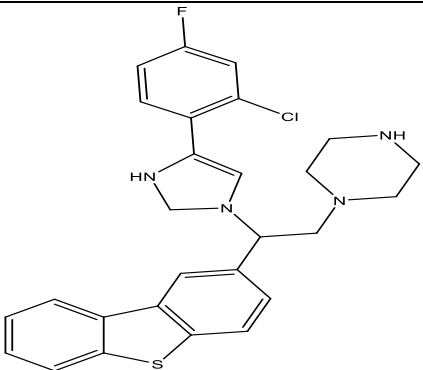
51		4.3534	4.4794	4.872	5.3914
52		4.3452	4.4825	4.118	4.6358
53		4.3407	4.4767	4.721	4.1250
54		4.3337	4.4715	4.019	4.3931

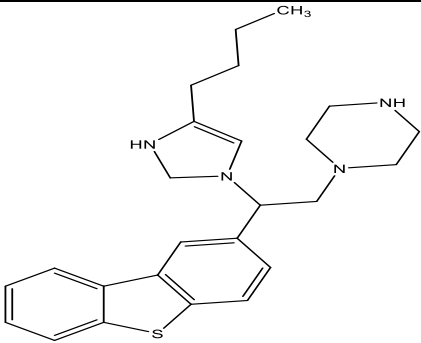
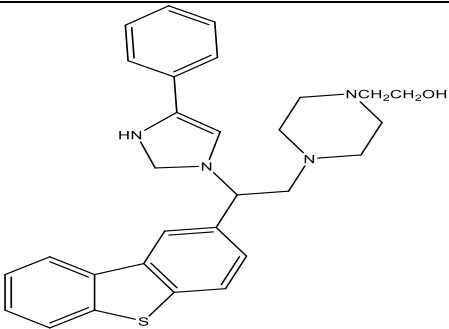
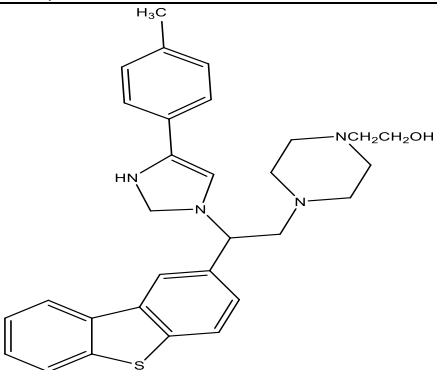
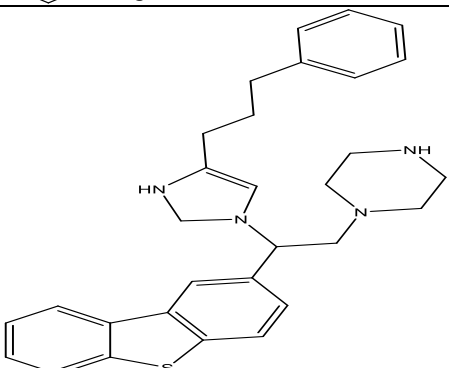
55		4.3493	4.4810	3.527	4.3762
56		4.3333	4.4741	4.387	3.6550
57		4.3369	4.4748	4.606	3.5770
58		4.3357	4.4788	4.269	4.6806

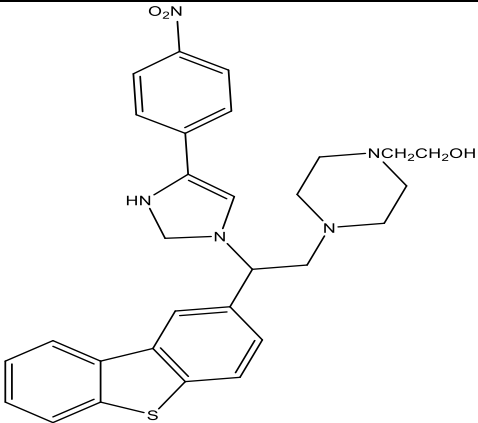
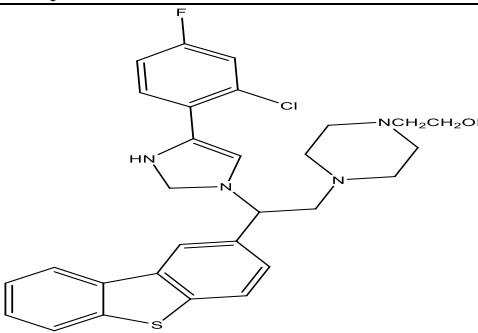
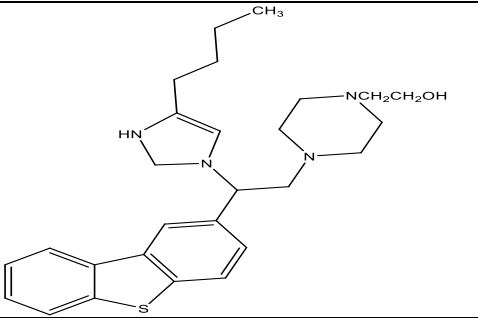
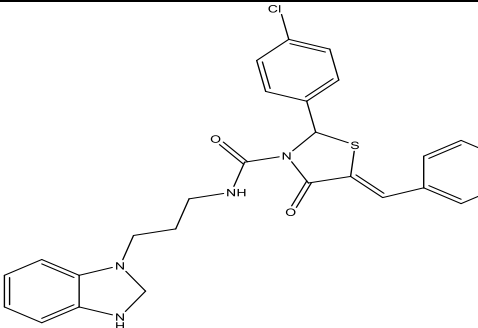
59		4.3387	4.4799	4.137	5.0128
60		4.3391	4.4841	4.116	3.0643
61		4.3340	4.4757	4.447	3.5384
62		4.3432	4.4760	4.193	4.3641

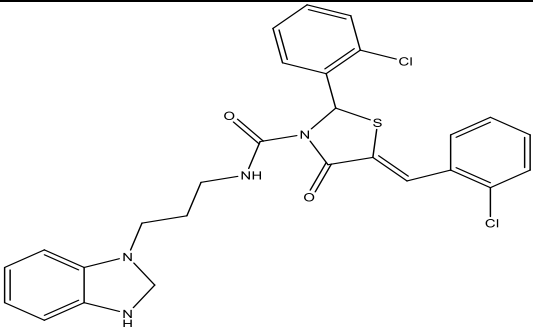
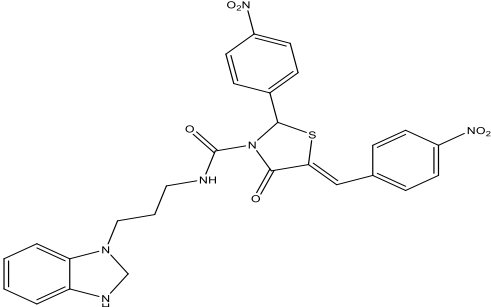
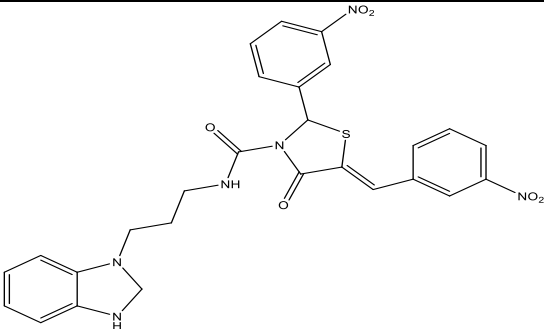
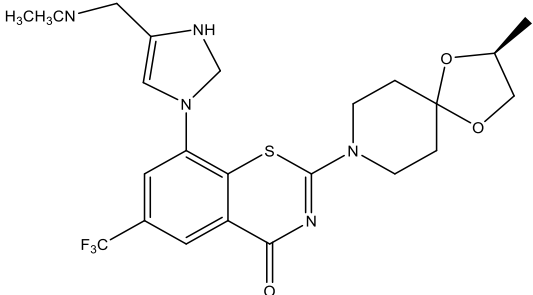
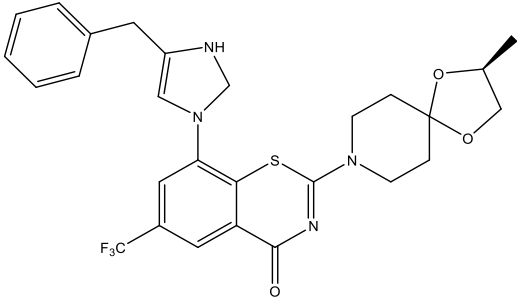
63		4.3346	4.4790	4.208	6.7577
64		4.3416	4.4826	4.032	7.5076
65		4.3332	4.4758	4.285	4.7628
66		4.3472	4.5061	4.814	6.6691

67		4.3332	4.4738	4.288	3.4100
68		4.3387	4.4736	4.415	4.0352
69		4.3325	4.4794	4.382	4.4156
70		4.3435	4.4735	4.514	3.2028

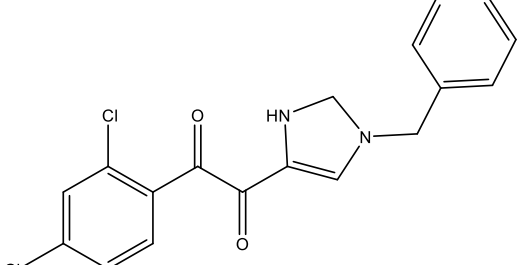
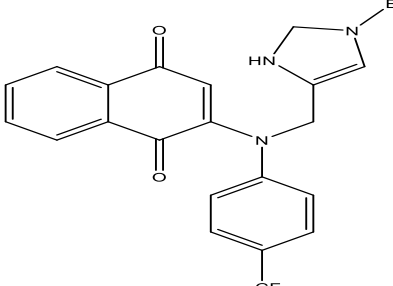
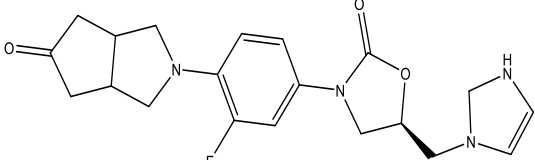
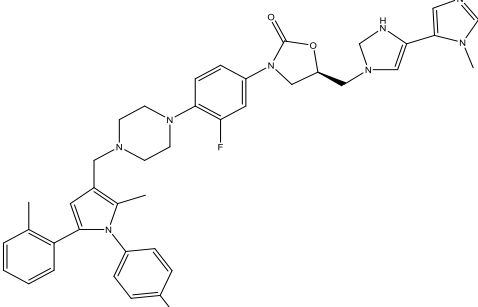
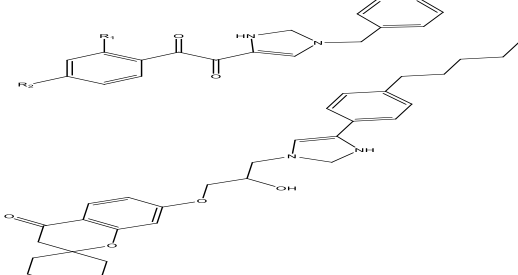
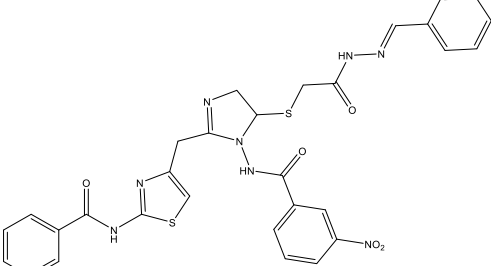
71		4.3430	4.4741	4.631	2.4690
72		4.3355	4.4757	4.338	4.2828
73		4.3354	4.4790	4.208	5.7021
74		4.3320	4.4763	4.556	5.7749

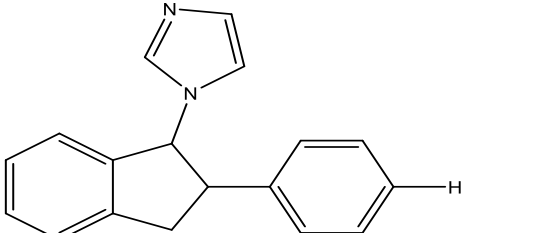
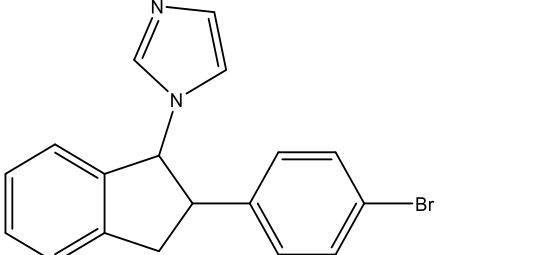
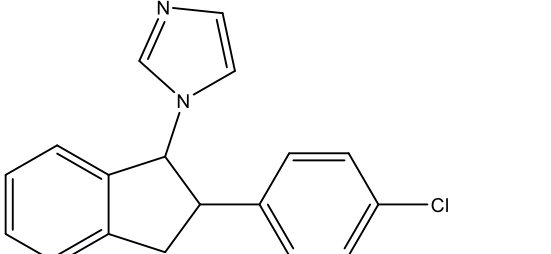
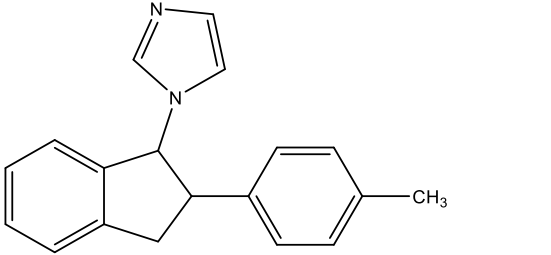
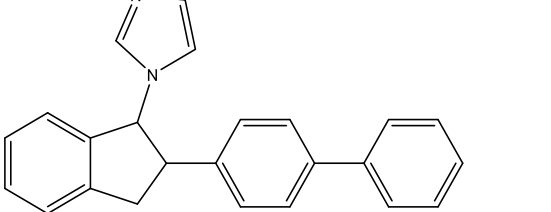
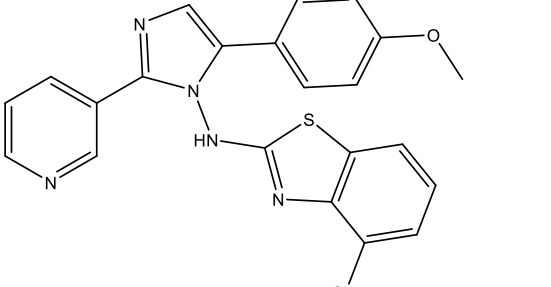
Shastri <i>et al.</i>	Journal of Drug Discovery and Therapeutics (JDDT)				
75		4.3352	4.4732	4.517	5.6609
76		4.3348	4.4773	4.433	4.9471
77		4.3306	4.4757	4.575	4.3661
78		4.3350	4.4759	4.428	6.7494

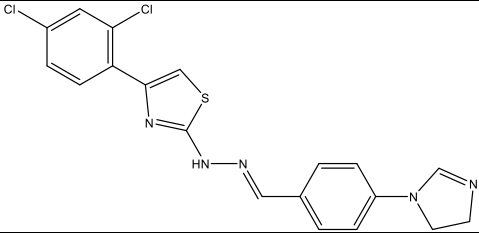
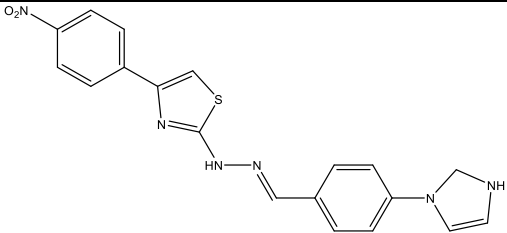
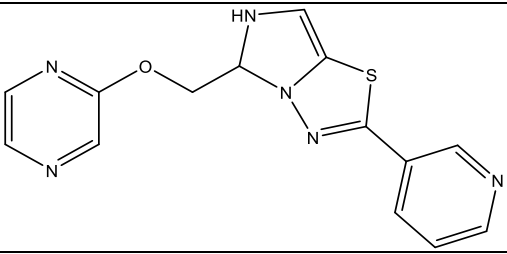
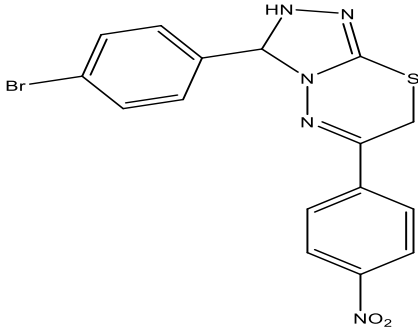
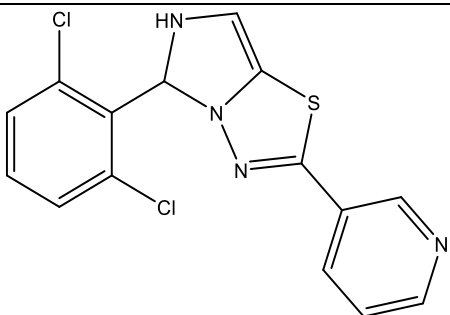
Shastri <i>et al.</i>	Journal of Drug Discovery and Therapeutics (JDDT)				
79		4.3378	4.4788	3.984	7.9638
80		4.3361	4.4719	4.629	7.1254
81		4.3276	4.4733	4.466	8.7375
82		4.3353	4.4772	4.246	7.0280

83		4.3350	4.4776	4.55	6.0740
84		4.3416	4.4835	3.873	4.5000
85		4.3405	4.4790	4.315	3.5902
86		4.3422	4.4739	4.069	5.7215
87		4.3419	4.4705	4.567	5.3869

153 | Page

Shastri <i>et al.</i>	Journal of Drug Discovery and Therapeutics (JDDT)				
94		4.3361	4.4733	4.567	5.1769
95		4.3407	4.4840	4.287	3.3925
96		4.3322	4.4787	4.412	6.3533
97		4.3330	4.4742	4.465	4.6248
98		4.3389	4.4815	4.032	6.7279
99		4.3357	4.4810	3.828	5.6288

Shastri <i>et al.</i>	Journal of Drug Discovery and Therapeutics (JDDT)				
100		4.3427	4.4730	4.575	6.8900
101		4.3413	4.4776	4.308	7.0763
102		4.3509	4.4830	4.563	3.4315
103		4.5241	4.1082	4.465	3.5404
104		4.3542	4.4651	4.638	6.6284
105		4.6365	4.4742	4.542	5.6307

106		4.3382	4.4187	4.467	2.5444
107		4.6262	4.4701	4.645	6.4544
108		4.5477	4.4958	4.530	5.5230
109		4.5651	4.4745	4.677	5.1745
110		4.3580	4.4654	4.547	2.5365

4 SUMMARY AND CONCLUSION:

The present work describes successfully applied QSAR study to characterize set of triazole derivatives and to identify essential structural requirements in 3D chemical space for the modulation and optimization of oxidoreductase inhibitor activity. The CoMFA, CoMSIA and HQSAR models showed meaningful statistical significance results in internal validation (q^2),

external validation (r^2) and predicted r^2 for triazole and 1,2,3-triazole and 1,2,4-triazole derivatives. The models generated through three layered QSAR approach exhibited reliable, ease correlative and predictive abilities. The explored CoMFA and CoMSIA models provided information about favorable and unfavorable region while HQSAR provides information about positive, negative and intermediate

contribution of sub-structural fingerprint requirements for imparting the biological activity. The CoMFA, CoMSIA and HQSAR contour maps revealed sufficient information to understand the structure-activity relationship (SAR) and to recognize structural features influencing inhibitory activity. Based on the SAR study generated by molecular modelling analysis, one hundred and two novel oxidoreductase inhibitor derivatives were successfully designed exhibiting moderate predicted activities in all three applied computational approaches.

The binding mode of the 1,2,3-triazole and 1,2,4-triazole analogues was clarified by the flexible docking method and Hydrogen bonding interaction and hydrophobic interaction were found to be important for the 1,2,3-triazole and 1,2,4-triazole analogues binding on PDB. Using the conformation generated from the docking study, highly predictive CoMFA and CoMSIA models were developed on 1,2,3-triazole analogue. The best derived CoMFA and CoMSIA model showed a predictive q^2 value for oxidoreductase inhibitor activity and the activities of compounds in the training set and test set were predicted with good accuracy.

The pharmacophore model developed helped us to obtain the common active pharmacophore regions along with the hydrophobe, donor and acceptor regions. All selected 1,2,3-triazole and 1,2,4-triazole analogues showed good alignment.

REFERENCES

1. Joule JA, Mills K. *Heterocyclic Chemistry*. 5th ed. Oxford: Wiley-Blackwell; 2010.
2. World Health Organization. Global Tuberculosis Report 2023 [Internet]. Geneva: WHO; 2023 [cited 2025 May 17]. Available from: <https://www.who.int/publications/i/item/9789240071887>
3. Leach AR. *Molecular Modelling: Principles and Applications*. 2nd ed. Harlow: Pearson Education Limited; 2001.
4. Jorgensen WL. The many roles of computation in drug discovery. *Science*. 2004;303(5665):1813-8. doi:10.1126/science.1096361
5. Wouters OJ, McKee M, Luyten J. Estimated research and development investment needed to bring a new medicine to market, 2009-2018. *Jama*. 2020 Mar 3;323(9):844-53.
6. Xie ZR, Hwang MJ. Methods for predicting protein-ligand binding sites. In *Molecular modeling of proteins* 2014 Sep 3 (pp. 383-398). New York, NY: Springer New York.
7. Goodford PJ. A computational procedure for determining energetically favorable binding sites on biologically important macromolecules. *Journal of medicinal chemistry*. 1985 Jul;28(7):849-57.
8. Böhm HJ. The computer program LUDI: a new method for the de novo design of enzyme inhibitors. *Journal of computer-aided molecular design*. 1992 Feb;6:61-78.
9. Choudhury C, Narahari Sastry G. Pharmacophore modelling and screening: concepts, recent developments and applications in rational drug design. *Structural bioinformatics: applications in preclinical drug discovery process*. 2019:25-53.
10. Yang SY. Pharmacophore modeling and applications in drug discovery: challenges and recent advances. *Drug discovery today*. 2010 Jun 1;15(11-12):444-50.
11. Huang N, Shoichet BK, Irwin JJ. Benchmarking sets for molecular docking. *Journal of medicinal chemistry*. 2006 Nov 16;49(23):6789-801.
12. Mysinger, M.M.; Carchia, M.; Irwin, J.J.; Shoichet, B.K. Directory of Useful Decoys, Enhanced (DUD-E): Better Ligands and Decoys for Better Benchmarking. *J. Med. Chem*. 2012, 55, 6582–6594.
13. Gaulton A, Hersey A, Nowotka M, Bento AP, Chambers J, Mendez D, Mutowo P, Atkinson F, Bellis LJ, Cibrián-Uhalte E, Davies M. The ChEMBL database in 2017. *Nucleic acids research*. 2017 Jan 4;45(D1):D945-54.
14. Wishart DS, Knox C, Guo AC, Cheng D, Shrivastava S, Tzur D, Gautam B, Hassanali M. DrugBank: a knowledgebase for drugs, drug actions and drug targets. *Nucleic acids research*. 2008 Jan 1;36(suppl_1):D901-6.
15. Wang Y, Bryant SH, Cheng T, Wang J, Gindulyte A, Shoemaker BA, Thiessen PA, He S, Zhang J. Pubchem bioassay: 2017 update. *Nucleic acids research*. 2017 Jan 4;45(D1):D955-63.

16. Gurung AB, Ali MA, Lee J, Farah MA, Al-Anazi KM. An updated review of computer-aided drug design and its application to COVID-19. *BioMed research international*. 2021;2021(1):8853056.
17. Seidel T, Ibis G, Bendix F, Wolber G. Strategies for 3D pharmacophore-based virtual screening. *Drug Discovery Today: Technologies*. 2010 Dec 1;7(4):e221-8.
18. Wolber G, Dornhofer AA, Langer T. Efficient overlay of small organic molecules using 3D pharmacophores. *Journal of computer-aided molecular design*. 2006 Dec;20(12):773-88.
19. Tyagi R, Singh A, Chaudhary KK, Yadav MK. Pharmacophore modeling and its applications. In *Bioinformatics 2022* Jan 1 (pp. 269-289). Academic Press.
20. Lill MA. Multi-dimensional QSAR in drug discovery. *Drug Discovery Today*. 2007 Dec 1;12(23-24):1013-7.
21. Triballeau N, Acher F, Brabet I, Pin JP, Bertrand HO. Virtual screening workflow development guided by the “receiver operating characteristic” curve approach. Application to high-throughput docking on metabotropic glutamate receptor subtype 4. *Journal of medicinal chemistry*. 2005 Apr 7;48(7):2534-47.
22. Mitra I, Saha A, Roy K. Pharmacophore mapping of arylamino-substituted benzo [b] thiophenes as free radical scavengers. *Journal of molecular modeling*. 2010 Oct;16(10):1585-96.
23. Koes DR, Camacho CJ. ZINCPharmer: pharmacophore search of the ZINC database. *Nucleic acids research*. 2012 May 2;40(W1):W409-14.
24. Lionta E, Spyrou G, K Vassilatis D, Cournia Z. Structure-based virtual screening for drug discovery: principles, applications and recent advances. *Current topics in medicinal chemistry*. 2014 Aug 1;14(16):1923-38.
25. Allen WJ, Balus TE, Mukherjee S, Brozell SR, Moustakas DT, Lang PT, Case DA, Kuntz ID, Rizzo RC. DOCK 6: Impact of new features and current docking performance. *Journal of computational chemistry*. 2015 Jun 5;36(15):1132-56.
26. Van De Waterbeemd H, Gifford E. ADMET in silico modelling: towards prediction paradise?. *Nature reviews Drug discovery*. 2003 Mar;2(3):192-204.
27. Kumar N, Hendriks BS, Janes KA, de Graaf D, Lauffenburger DA. Applying computational modeling to drug discovery and development. *Drug discovery today*. 2006 Sep 1;11(17-18):806-11.
28. Oprea TI, Matter H. Integrating virtual screening in lead discovery. *Current opinion in chemical biology*. 2004 Aug 1;8(4):349-58.
29. Chin DN, Chuaqui CE, Singh J. Integration of virtual screening into the drug discovery process. *Mini Reviews in Medicinal Chemistry*. 2004 Dec 1;4(10):1053-65.
30. Jain AN. Virtual screening in lead discovery and optimization. *Current opinion in drug discovery & development*. 2004 Jul 1;7(4):396-403.
31. Stahl M, Guba W, Kansy M. Integrating molecular design resources within modern drug discovery research: the Roche experience. *Drug discovery today*. 2006 Apr 1;11(7-8):326-33.
32. Dror O, Shulman-Peleg A, Nussinov R, Wolfson HJ. Predicting molecular interactions in silico: I. A guide to pharmacophore identification and its applications to drug design. *Current medicinal chemistry*. 2004 Jan 1;11(1):71-90.
33. Schneidman-Duhovny D, Nussinov R, Wolfson HJ. Predicting molecular interactions in silico: II. Protein-protein and protein-drug docking. *Current medicinal chemistry*. 2004 Jan 1;11(1):91-107.
34. Toba S, Srinivasan J, Maynard AJ, Sutter J. Using pharmacophore models to gain insight into structural binding and virtual screening: an application study with CDK2 and human DHFR. *Journal of chemical information and modeling*. 2006 Mar 27;46(2):728-35.
35. Toba S, Srinivasan J, Maynard AJ, Sutter J. Using pharmacophore models to gain insight into structural binding and virtual screening: an application study with CDK2 and human DHFR. *Journal of chemical information and modeling*. 2006 Mar 27;46(2):728-35.
36. Funk OF, Kettmann V, Drimal J, Langer T. Chemical function based pharmacophore generation of endothelin-A selective

- receptor antagonists. *Journal of medicinal chemistry*. 2004 May 20;47(11):2750-60.
37. Funk OF, Kettmann V, Drimal J, Langer T. Chemical function based pharmacophore generation of endothelin-A selective receptor antagonists. *Journal of medicinal chemistry*. 2004 May 20;47(11):2750-60.
38. Gurung AB, Ali MA, Lee J, Farah MA, Al-Anazi KM. An updated review of computer-aided drug design and its application to COVID-19. *BioMed research international*. 2021;2021(1):8853056.
39. Seidel T, Ibis G, Bendix F, Wolber G. Strategies for 3D pharmacophore-based virtual screening. *Drug Discovery Today: Technologies*. 2010 Dec 1;7(4):e221-8.
40. Wolber G, Dornhofer AA, Langer T. Efficient overlay of small organic molecules using 3D pharmacophores. *Journal of computer-aided molecular design*. 2006 Dec;20(12):773-88.
41. Tyagi R, Singh A, Chaudhary KK, Yadav MK. Pharmacophore modeling and its applications. In *Bioinformatics 2022* Jan 1 (pp. 269-289). Academic Press.
42. Lill MA. Multi-dimensional QSAR in drug discovery. *Drug Discovery Today*. 2007 Dec 1;12(23-24):1013-7.
43. Sadineni K, Reddy Basireddy S, Rao Allaka T, Yatam S, Bhoomandla S, Muvvala V, Babu Haridasam S. Design, Synthesis and In vitro Antitubercular Effect of New Chalcone Derivatives Coupled with 1, 2, 3-Triazoles: A Computational Docking Techniques. *Chemistry & Biodiversity*. 2024 May;21(5):e202400389.
44. Baddam SR, Avula MK, Akula R, Battula VR, Kalagara S, Buchikonda R, Ganta S, Venkatesan S, Allaka TR. Design, synthesis and in silico molecular docking evaluation of novel 1, 2, 3-triazole derivatives as potent antimicrobial agents. *Heliyon*. 2024 Apr 15;10(7).
45. El Faydy M, Lakhrissi L, Dahaieh N, Ounine K, Tüzün B, Chahboun N, Boshala A, AlObaid A, Warad I, Lakhrissi B, Zarrouk A. Synthesis, biological properties, and molecular docking study of novel 1, 2, 3-triazole-8-quinolinol hybrids. *ACS omega*. 2024 May 31;9(23):25395-409.
46. Bouamrane S, Khaldan A, Alaqrbeh M, Sbair A, Ajana MA, Lakhli T, Bouachrine M, Maghat H. Computational integration for antifungal 1, 2, 4-triazole inhibitors design: QSAR, molecular docking, molecular dynamics simulations, ADME/Tox, and retrosynthesis studies. *Chemical Physics Impact*. 2024 Jun 1;8:100502.
47. Dong Y, Li M, Hao Y, Feng Y, Ren Y, Ma H. Antifungal activity, structure-activity relationship and molecular docking studies of 1, 2, 4-triazole schiff base derivatives. *Chemistry & Biodiversity*. 2023 Mar;20(3):e202201107.
48. Şahin İ, Çeşme M, Özgeriş FB, Tümer F. Triazole based novel molecules as potential therapeutic agents: Synthesis, characterization, biological evaluation, in-silico ADME profiling and molecular docking studies. *Chemico-Biological Interactions*. 2023 Jan 25;370:110312.
49. Jawad WA, Balakit AA, Al-Jibouri MN, Sert Y, Obies M. Design, synthesis, characterization, antioxidant, antiproliferative activity and molecular docking studies of new transition metal complexes of 1, 2, 4-triazole as combretastatin A-4 analogues. *Journal of Molecular Structure*. 2023 Feb 15;1274:134437.
50. Göktürk T, Sakallı Çetin E, Hökelek T, Pekel H, Şensoy O, Aksu EN, Gup R. Synthesis, structural investigations, DNA/BSA interactions, molecular docking studies, and anticancer activity of a new 1, 4-disubstituted 1, 2, 3-triazole derivative. *ACS omega*. 2023 Aug 25;8(35):31839-56.
51. Anwer KE, Sayed GH, Ramadan RM. Synthesis, spectroscopic, DFT calculations, biological activities and molecular docking studies of new isoxazolone, pyrazolone, triazine, triazole and amide derivatives. *Journal of Molecular Structure*. 2022 May 15;1256:132513.
52. Alhamzani AG, Yousef TA, Abou-Krishna MM, Raghu MS, Kumar KY, Prashanth MK, Jeon BH. Design, synthesis, molecular docking and pharmacological evaluation of novel triazine-based triazole derivatives as potential anticonvulsant agents. *Bioorganic*

- & Medicinal Chemistry Letters. 2022 Dec 1;77:129042.
53. Nural Y, Ozdemir S, Yalcin MS, Demir B, Atabey H, Seferoglu Z, Ece A. New bis-and tetrakis-1, 2, 3-triazole derivatives: Synthesis, DNA cleavage, molecular docking, antimicrobial, antioxidant activity and acid dissociation constants. *Bioorganic & Medicinal Chemistry Letters*. 2022 Jan 1;55:128453.
54. İslamoğlu F, Hacifazlıoğlu E. Investigation of the usability of some triazole derivative compounds as drug active ingredients by ADME and molecular docking properties. *Moroccan Journal of Chemistry*. 2022 May 26;10(4):J-Chem.
55. Kumar VS, Mary YS, Mary YS, Serdaroğlu G, Rad AS, Roxy MS, Manjula PS, Sarojini BK. Conformational analysis and DFT investigations of two triazole derivatives and its halogenated substitution by using spectroscopy, AIM and molecular docking. *Chemical Data Collections*. 2021 Feb 1;31:100625.
56. Nunes PS, da Silva G, Nascimento S, Mantoani SP, de Andrade P, Bernardes ES, Kawano DF, Leopoldino AM, Carvalho I. Synthesis, biological evaluation and molecular docking studies of novel 1, 2, 3-triazole-quinazolines as antiproliferative agents displaying ERK inhibitory activity. *Bioorganic Chemistry*. 2021 Aug 1;113:104982.
57. Nehra N, Tittal RK, Ghule VD. 1, 2, 3-Triazoles of 8-hydroxyquinoline and HBT: Synthesis and studies (DNA binding, antimicrobial, molecular docking, ADME, and DFT). *ACS omega*. 2021 Oct 6;6(41):27089-100.
58. Kumar CP, Prathibha BS, Prasad KN, Raghu MS, Prashanth MK, Jayanna BK, Alharthi FA, Chandrasekhar S, Revanasiddappa HD, Kumar KY. Click synthesis of 1, 2, 3-triazole based imidazoles: Antitubercular evaluation, molecular docking and HSA binding studies. *Bioorganic & Medicinal Chemistry Letters*. 2021 Mar 15;36:127810.
59. Ganesh N, Singh M, Chandrashekar VM, Pujar GV. Antitubercular potential of novel isoxazole encompassed 1, 2, 4-triazoles: design, synthesis, molecular docking study and evaluation of antitubercular activity. *Anti-Infective Agents*. 2021 Apr 1;19(2):147-61.
60. Özil M, Tacal G, Baltaş N, Emirik M. Synthesis and molecular docking studies of novel triazole derivatives as antioxidant agents. *Letters in Organic Chemistry*. 2020 Apr 1;17(4):309-20.
61. Turkey A, Sherbiny FF, Bayoumi AH, Ahmed HE, Abulkhair HS. Novel 1, 2, 4-triazole derivatives: Design, synthesis, anticancer evaluation, molecular docking, and pharmacokinetic profiling studies. *Archiv der Pharmazie*. 2020 Dec;353(12):2000170.
62. Gökalp M, Dede B, Tilki T, Atay ÇK. Triazole based azo molecules as potential antibacterial agents: Synthesis, characterization, DFT, ADME and molecular docking studies. *Journal of Molecular Structure*. 2020 Jul 15;1212:128140.
63. Karczmarzyk Z, Swatko-Ossor M, Wysocki W, Drozd M, Ginalska G, Pachuta-Stec A, Pitucha M. New application of 1, 2, 4-triazole derivatives as antitubercular agents. Structure, in vitro screening and docking studies. *Molecules*. 2020 Dec 19;25(24):6033.
64. Pal T, Bhimaneni S, Sharma A, Flora SJ. Design, synthesis, biological evaluation and molecular docking study of novel pyridoxine-triazoles as anti-Alzheimer's agents. *RSC advances*. 2020;10(44):26006-21.
65. Chauhan S, Verma V, Kumar D, Kumar A. Synthesis, antimicrobial evaluation and docking study of triazole containing triaryl-1 H-imidazole. *Synthetic Communications*. 2019 Jun 3;49(11):1427-35.
66. Hussain M, Qadri T, Hussain Z, Saeed A, Channar PA, Shehzadi SA, Hassan M, Larik FA, Mahmood T, Malik A. Synthesis, antibacterial activity and molecular docking study of vanillin derived 1, 4-disubstituted 1, 2, 3-triazoles as inhibitors of bacterial DNA synthesis. *Heliyon*. 2019 Nov 1;5(11).
67. Thanh ND, Ha NT, Le CT, Van HT, Toan VN, Toan DN, Dang LH. Synthesis, biological evaluation and molecular docking study of 1, 2, 3-1H-triazoles having 4H-

- pyrano [2, 3-d] pyrimidine as potential Mycobacterium tuberculosis protein tyrosine phosphatase B inhibitors. *Bioorganic & medicinal chemistry letters*. 2019 Jan 15;29(2):164-71.
68. Phatak PS, Bakale RD, Dhumal ST, Dahiawade LK, Choudhari PB, Siva Krishna V, Sriram D, Haval KP. Synthesis, antitubercular evaluation and molecular docking studies of phthalimide bearing 1, 2, 3-triazoles. *Synthetic communications*. 2019 Aug 18;49(16):2017-28.
69. Shaikh MH, Subhedar DD, Nawale L, Sarkar D, Khan FA, Sangshetti JN, Shingate BB. Novel benzylidenehydrazide-1, 2, 3-triazole conjugates as antitubercular agents: synthesis and molecular docking. *Mini Reviews in Medicinal Chemistry*. 2019 Aug 1;19(14):1178-94.
70. Reddyrajula R, Dalimba U. Quinoline-1, 2, 3-triazole hybrids: design and synthesis through click reaction, evaluation of anti-tubercular activity, molecular docking and in silico ADME studies. *ChemistrySelect*. 2019 Mar 7;4(9):2685-93.
71. Wu J, Ni T, Chai X, Wang T, Wang H, Chen J, Jin Y, Zhang D, Yu S, Jiang Y. Molecular docking, design, synthesis and antifungal activity study of novel triazole derivatives. *European journal of medicinal chemistry*. 2018 Jan 1;143:1840-6.
72. Khare SP, Deshmukh TR, Sangshetti JN, Krishna VS, Sriram D, Khedkar VM, Shingate BB. Design, synthesis and molecular docking studies of novel triazole-chromene conjugates as antitubercular, antioxidant and antifungal agents. *ChemistrySelect*. 2018 Dec 13;3(46):13113-22.
73. Danne AB, Choudhari AS, Chakraborty S, Sarkar D, Khedkar VM, Shingate BB. Triazole-diindolylmethane conjugates as new antitubercular agents: synthesis, bioevaluation, and molecular docking. *MedChemComm*. 2018;9(7):1114-30.
74. Savanur HM, Naik KN, Ganapathi SM, Kim KM, Kalkhambkar RG. Click chemistry inspired design, synthesis and molecular docking studies of coumarin, quinolinone linked 1, 2, 3-triazoles as promising anti-microbial agents. *ChemistrySelect*. 2018 May 24;3(19):5296-303.
75. Mustafa M, Abdelhamid D, Abdelhafez EM, Ibrahim MA, Gamal-Eldeen AM, Aly OM. Synthesis, antiproliferative, anti-tubulin activity, and docking study of new 1, 2, 4-triazoles as potential combretastatin analogues. *European journal of medicinal chemistry*. 2017 Dec 1;141:293-305.
76. Zhang HJ, Wang XZ, Cao Q, Gong GH, Quan ZS. Design, synthesis, anti-inflammatory activity, and molecular docking studies of perimidine derivatives containing triazole. *Bioorganic & Medicinal Chemistry Letters*. 2017 Sep 15;27(18):4409-14.
77. Naidu KM, Srinivasarao S, Agnieszka N, Ewa AK, Kumar MM, Sekhar KV. Seeking potent anti-tubercular agents: Design, synthesis, anti-tubercular activity and docking study of various ((triazoles/indole)-piperazin-1-yl/1, 4-diazepan-1-yl) benzo [d] isoxazole derivatives. *Bioorganic & medicinal chemistry letters*. 2016 May 1;26(9):2245-50.
78. Shaikh MH, Subhedar DD, Arkile M, Khedkar VM, Jadhav N, Sarkar D, Shingate BB. Synthesis and bioactivity of novel triazole incorporated benzothiazinone derivatives as antitubercular and antioxidant agent. *Bioorganic & medicinal chemistry letters*. 2016 Jan 15;26(2):561-9.
79. Shaikh MH, Subhedar DD, Nawale L, Sarkar D, Khan FA, Sangshetti JN, Shingate BB. 1, 2, 3-Triazole derivatives as antitubercular agents: synthesis, biological evaluation and molecular docking study. *MedChemComm*. 2015;6(6):1104-16.
80. Anand A, Naik RJ, Revankar HM, Kulkarni MV, Dixit SR, Joshi SD. A click chemistry approach for the synthesis of mono and bis aryloxy linked coumarinyl triazoles as anti-tubercular agents. *European journal of medicinal chemistry*. 2015 Nov 13;105:194-207.
81. Seeka S, Narsimha S, Savitha Jyostna T, Reddy NV. Synthesis, antibacterial, and molecular docking study of some novel 1, 2, 3-triazole derivatives. *International Journal of Pharmacology*. 2015;2(4):26-32.

82. Negi B, Raj KK, Siddiqui SM, Ramachandran D, Azam A, Rawat DS. In vitro antiamoebic activity evaluation and docking studies of metronidazole–triazole hybrids. *ChemMedChem*. 2014 Nov;9(11):2439-44.
83. Kumar D, Khare G, Kidwai S, Tyagi AK, Singh R, Rawat DS. Synthesis of novel 1, 2, 3-triazole derivatives of isoniazid and their in vitro and in vivo antimycobacterial activity evaluation. *European journal of medicinal chemistry*. 2014 Jun 23;81:301-13.
84. Pingaew R, Saekee A, Mandi P, Nantasenamat C, Prachayasittikul S, Ruchirawat S, Prachayasittikul V. Synthesis, biological evaluation and molecular docking of novel chalcone–coumarin hybrids as anticancer and antimalarial agents. *European Journal of Medicinal Chemistry*. 2014 Oct 6;85:65-76.
85. Zhang S, Xu Z, Gao C, Ren QC, Chang L, Lv ZS, Feng LS. Triazole derivatives and their anti-tubercular activity. *European journal of medicinal chemistry*. 2017 Sep 29;138:501-13.
86. Klebe G, Abraham U & Mietzner T. Molecular similarity indices in a comparative analysis (CoMSIA) of drug molecules to correlate and predict their biological activity. *Journal of Medicinal Chemistry*. 37, 1994, 4130-4146.
87. Sridhara J, Foroozesh M & Stevens K. A QSAR models of cytochrome P450 enzyme 1A2 inhibitors using CoMFA, CoMSIA and HQSAR. *SAR and QSAR in Environmental Research*. 22, 2011, 681-697.
88. Zoltewicz J & Deady W. Quaternization of Heteroaromatic Compounds. *Quantitative Aspects. Advances in Heterocyclic Chemistry. Advances in Heterocyclic Chemistry*. 22, 1978, 71–121.
89. Kini SG, Bhat AR, Bryant B, Williamson JS, Dayan FE. Synthesis, antitubercular activity and docking study of novel cyclic azole substituted diphenyl ether derivatives. *European journal of medicinal chemistry*. 2009 Feb 1;44(2):492-500.
90. Thomas KD, Adhikari AV, Telkar S, Chowdhury IH, Mahmood R, Pal NK, Row G, Sumesh E. Design, synthesis and docking studies of new quinoline-3-carbohydrazide derivatives as antitubercular agents. *European journal of medicinal chemistry*. 2011 Nov 1;46(11):5283-92.
91. Mohan SB, Kumar BR, Dinda SC, Naik D, Seenivasan SP, Kumar V, Rana DN, Brahmshatriya PS. Microwave-assisted synthesis, molecular docking and antitubercular activity of 1, 2, 3, 4-tetrahydropyrimidine-5-carbonitrile derivatives. *Bioorganic & medicinal chemistry letters*. 2012 Dec 15;22(24):7539-42.
92. Saikia N, Rajkhowa S, Deka RC. Density functional and molecular docking studies towards investigating the role of single-wall carbon nanotubes as nanocarrier for loading and delivery of pyrazinamide antitubercular drug onto pncA protein. *Journal of computer-aided molecular design*. 2013 Mar 1;27(3):257-76.
93. Yadav DK, Ahmad I, Shukla A, Khan F, Negi AS, Gupta A. QSAR and docking studies on chalcone derivatives for antitubercular activity against *M. tuberculosis* H37Rv. *Journal of Chemometrics*. 2014 Jun;28(6):499-507.
94. Pulaganti M, Banaganapalli B, Mulakayala C, Chitta SK, Anuradha CM. Molecular modeling and docking studies of O-succinylbenzoate synthase of *M. tuberculosis*—a potential target for antituberculosis drug design. *Applied biochemistry and biotechnology*. 2014 Feb 1;172(3):1407-32.
95. Desai NC, Somani H, Trivedi A, Bhatt K, Nawale L, Khedkar VM, Jha PC, Sarkar D. Synthesis, biological evaluation and molecular docking study of some novel indole and pyridine based 1, 3, 4-oxadiazole derivatives as potential antitubercular agents. *Bioorganic & medicinal chemistry letters*. 2016 Apr 1;26(7):1776-83.
96. Blake L, Soliman ME. Identification of irreversible protein splicing inhibitors as potential anti-TB drugs: insight from hybrid non-covalent/covalent docking virtual screening and molecular dynamics simulations. *Medicinal Chemistry Research*. 2014 May 1;23(5):2312-23.

97. Khedr MA, Pillay M, Chandrashekharappa S, Chopra D, Aldhubiab BE, Attimarad M, Alwassil OI, Mlisana K, Odhav B, Venugopala KN. Molecular modeling studies and anti-TB activity of trisubstituted indolizine analogues; molecular docking and dynamic inputs. *Journal of Biomolecular Structure and Dynamics*. 2018 Jun 11;36(8):2163-78.
98. Dandawate P, Vemuri K, Swamy KV, Khan EM, Sritharan M, Padhye S. Synthesis, characterization, molecular docking and anti-tubercular activity of Plumbagin-Isoniazid Analog and its β -cyclodextrin conjugate. *Bioorganic & Medicinal Chemistry Letters*. 2014 Nov 1;24(21):5070-5.
99. Barot KP, Jain SV, Gupta N, Kremer L, Singh S, Takale VB, Joshi K, Ghate MD. Design, synthesis and docking studies of some novel (R)-2-(4'-chlorophenyl)-3-(4'-nitrophenyl)-1, 2, 3, 5-tetrahydrobenzo [4, 5] imidazo [1, 2-c] pyrimidin-4-ol derivatives as antitubercular agents. *European Journal of Medicinal Chemistry*. 2014 Aug 18;83:245-55.
100. Balaji NV, Babu BH, Subbaraju GV, Nagasree KP, Kumar MM. Synthesis, screening and docking analysis of hispolon analogs as potential antitubercular agents. *Bioorganic & Medicinal Chemistry Letters*. 2017 Jan 1;27(1):11-5.
101. Chaitanya M, Babajan B, Anuradha CM, Naveen M, Rajasekhar C, Madhusudana P, Kumar CS. Exploring the molecular basis for selective binding of Mycobacterium tuberculosis Asp kinase toward its natural substrates and feedback inhibitors: a docking and molecular dynamics study. *Journal of molecular modeling*. 2010 Aug 1;16(8):1357-67.
102. Anuradha CM, Mulakayala C, Babajan B, Naveen M, Rajasekhar C, Kumar CS. Probing ligand binding modes of Mycobacterium tuberculosis MurC ligase by molecular modeling, dynamics simulation and docking. *Journal of molecular modeling*. 2010 Jan 1;16(1):77-85.
103. Joshi SD, Dixit SR, Kirankumar MN, Aminabhavi TM, Raju KV, Narayan R, Lherbet C, Yang KS. Synthesis, antimycobacterial screening and ligand-based molecular docking studies on novel pyrrole derivatives bearing pyrazoline, isoxazole and phenyl thiourea moieties. *European journal of medicinal chemistry*. 2016 Jan 1;107:133-52.
104. Desai NC, Trivedi AR, Khedkar VM. Preparation, biological evaluation and molecular docking study of imidazolyl dihydropyrimidines as potential Mycobacterium tuberculosis dihydrofolate reductase inhibitors. *Bioorganic & medicinal chemistry letters*. 2016 Aug 15;26(16):4030-5.
105. Sengupta S, Roy D, Bandyopadhyay S. Structural insight into Mycobacterium tuberculosis maltosyl transferase inhibitors: pharmacophore-based virtual screening, docking, and molecular dynamics simulations. *Journal of Biomolecular Structure and Dynamics*. 2015 Dec 2;33(12):2655-66.
106. Martins F, Santos S, Ventura C, Elvas-Leitão R, Santos L, Vitorino S, Reis M, Miranda V, Correia HF, Aires-de-Sousa J, Kovalishyn V. Design, synthesis and biological evaluation of novel isoniazid derivatives with potent antitubercular activity. *European journal of medicinal chemistry*. 2014 Jun 23;81:119-38.
107. Koch O, Jäger T, Heller K, Khandavalli PC, Pretzel J, Becker K, Flohé L, Selzer PM. Identification of M. tuberculosis thioredoxin reductase inhibitors based on high-throughput docking using constraints. *Journal of Medicinal Chemistry*. 2013 Jun 27;56(12):4849-59.
108. Naqvi A, Malasoni R, Srivastava A, Pandey RR, Dwivedi AK. Design, synthesis and molecular docking of substituted 3-hydrazinyl-3-oxo-propanamides as anti-tubercular agents. *Bioorganic & medicinal chemistry letters*. 2014 Nov 15;24(22):5181-4.
109. Al-Tamimi AM, Mary YS, Miniya PB, Al-Wahaibi LH, El-Emam AA, Armaković S, Armaković SJ. Synthesis, spectroscopic analyses, chemical reactivity and molecular docking study and anti-tubercular activity of pyrazine and condensed oxadiazole

- derivatives. *Journal of Molecular Structure*. 2018 Jul 15;1164:459-69.
110. Jose G, Kumara TH, Sowmya HB, Sriram D, Row TN, Hosamani AA, More SS, Janardhan B, Harish BG, Telkar S, Ravikumar YS. Synthesis, molecular docking, antimycobacterial and antimicrobial evaluation of new pyrrolo [3, 2-c] pyridine Mannich bases. *European Journal of Medicinal Chemistry*. 2017 May 5;131:275-88.
111. Singh N, Tiwari S, Srivastava KK, Siddiqi MI. Identification of novel inhibitors of *Mycobacterium tuberculosis* PknG using pharmacophore based virtual screening, docking, molecular dynamics simulation, and their biological evaluation. *Journal of Chemical Information and Modeling*. 2015 Jun 22;55(6):1120-9.
112. Agrawal KM, Talele GS. Synthesis and antibacterial, antimycobacterial and docking studies of novel N-piperazinyl fluoroquinolones. *Medicinal Chemistry Research*. 2013 Feb 1;22(2):818-31.
113. Sengupta S, Roy D, Bandyopadhyay S. Structural insight into *Mycobacterium tuberculosis* maltosyl transferase inhibitors: pharmacophore-based virtual screening, docking, and molecular dynamics simulations. *Journal of Biomolecular Structure and Dynamics*. 2015 Dec 2;33(12):2655-66.
114. Zhang J, Zhao J, Wang L, Liu J, Ren D, Ma Y. Design, synthesis and docking studies of some spiro-oxindole dihydroquinazolinones as antibacterial agents. *Tetrahedron*. 2016 Feb 18;72(7):936-43.
115. Saxena S, Abdullah M, Sriram D, Guruprasad L. Discovery of novel inhibitors of *Mycobacterium tuberculosis* MurG: Homology modelling, structure based pharmacophore, molecular docking, and molecular dynamics simulations. *Journal of Biomolecular Structure and Dynamics*. 2018 Sep 10;36(12):3184-98.
116. Kumar M, Vijayakrishnan R, Rao GS. In silico structure-based design of a novel class of potent and selective small peptide inhibitor of *Mycobacterium tuberculosis* Dihydrofolate reductase, a potential target for anti-TB drug discovery. *Molecular diversity*. 2010 Aug 1;14(3):595-604.
117. El-Azab AS, Mary YS, Abdel-Aziz AA, Miniyar PB, Armaković S, Armaković SJ. Synthesis, spectroscopic analyses (FT-IR and NMR), vibrational study, chemical reactivity and molecular docking study and anti-tubercular activity of condensed oxadiazole and pyrazine derivatives. *Journal of Molecular Structure*. 2018 Mar 15;1156:657-74.
118. Pulaganti M, Banaganapalli B, Mulakayala C, Chitta SK, Anuradha CM. Molecular modeling and docking studies of O-succinylbenzoate synthase of *M. tuberculosis*—a potential target for antituberculosis drug design. *Applied biochemistry and biotechnology*. 2014 Feb 1;172(3):1407-32.
119. H.N. Nagesh, K.M. Naidu, D.H. Rao, J.P. Sridevi, D. Sriram, P. Yogeewari, K.V. Gowri, C. Sekhar, *Bioorg. Med. Chem. Lett*. 23 (2013) 6805e6810.
120. K.D. Thomas, A.V. Adhikari, I.H. Chowdhury, E. Sumesh, N.K. Pal, *Eur. J. Med. Chem.* 46 (2011) 2503e2512.